Vortex detection through pressure measurements

Aditi Bhide

A thesis

submitted in partial fulfillment of the

requirements for the degree of

Master of Science in Aeronautics & Astronautics

University of Washington

2016

Committee:

Carl Knowlen

James C. Hermanson

Program authorized to offer degree:

Aeronautics and Astronautics

University of Washington

Abstract

Vortex detection through pressure measurements

Aditi Bhide

Chair of Supervisory Committee:
Professor Carl Knowlen
Aeronautics & Astronautics

Vortex Generators (VGs) are known to hinder boundary layer separation, a frequently unwanted phenomenon when it comes to external flows over aircraft wings, on-ground vehicles or internal flows within pipes, diffusers and turbomachinery. Boundary layer separation leads to loss of lift, higher drag and subsequently, energy losses. The vortices generated inhibit boundary layer separation. This thesis is an effort to discern the strength and location of these generated vortices using an array of VGs over a flat plate. Such information may be useful in the future in active control systems for streamwise vortices, which have been proposed to relaminarize turbulent boundary layers. Flow over flat plates, simulated using wind tunnel experiments, is studied for pressure variation using an array of pressure ports mounted over the plate and connected to suitable pressure sensors. Pressure coefficient and Velocity maps are generated using the data obtained from the Kirsten Wind Tunnel data acquisition system. These represent the nature of the flow field over the plate and are used to locate the vortices and determine their strength. It was found that the vortices can be detected using this method and their strength and location can be estimated.

Table of Contents

Nomenclature

C_p = Pressure coefficient

p = pressure at ports

p_∞ = ambient pressure

ρ = air density

V_∞ = Wind Velocity

c = Vortex generator chord length

h = Vortex generator height

β = Vortex generator angle of attack

α = Mounting Angle on plate

t = Vortex generator thickness

$V = \omega$ = Vorticity

δ = Boundary layer thickness

$C = \Gamma$ = Circulation

List of Figures

List of Tables

Acknowledgements

I will forever be grateful to Dr. Robert E. Breidenthal and Dr. Giovanni Nino for letting me be a part of their research group. It was a massive learning experience and this thesis is a manifestation of the inspiration and encouragement I received from them to make me understand every facet and dimension of the project. Without their efforts, I would have never been able to learn this much in the last year and a half.

I would like to express my sincere thanks to Dr. Knowlen and Dr. Hermanson for being a part of the thesis review committee and for their constant support and patience with the countless drafts and edits.

I also express my gratitude towards Ms. Fiona Spencer and Mr. Dzung Tran for being the guides and helping me set up my experiments. Similarly, I cannot thank enough Mr. Jack Ross and the Kirsten Wind Tunnel crew for being accommodating and understanding about my experiment goals and letting me test at Kirsten in extremely limited time I had.

My peers from the research group, the fellow students I met at the AA Department and all my friends in Seattle, you all are nothing less than a family away from home and a big thank you for that!

Lastly and most importantly, thank you so much Aai and Baba, for believing in me always. I would not be writing this had it not been for you both.

Chapter I

Introduction

The turn of this century has seen large scale improvements in flight technology. Design optimization is being used continuously to increase speed and efficiency and reduce aerodynamic drag in transport applications. But hand in hand with these improvements, there is also a steady rise in fuel oil prices owing to depleting resources with increasing environmental concerns involving toxic exhausts and greenhouse gases. This thesis explores a method to combat a fundamental aerodynamic problem, which if solved can reduce fuel consumption and increase speed of travel and its efficiency. Flow separation in a boundary layer is a phenomenon which ups the aerodynamic drag. This thesis reports on an experimental wind tunnel study which aims to locate the vortices formed due to Vortex Generators (VGs), using an array of pressure sensors. VGs are used commonly on aerodynamic surfaces to reduce/do away with flow separation. It is important to know the location and strength of the vortices formed in order to efficiently reduce flow separation. It may also be used as part of an active control system for stationary vortices to relaminarize turbulent boundary layers.

This introductory chapter aims to highlight the concepts used in the study. These include some fundamental fluid mechanics definitions as well as the key topics specific to this study. Chapter II looks into the literature resources that were referred to find the inspiration, background, and the direction to conduct the experiments and draw comparative inferences. Chapter III deals with the experimental setup and information about the technical specifications that were required to be met in order to obtain the desired results. The results is what the Chapter IV delves into. A compilation of the graphs, plots and images obtained after processing the Wind Tunnel data in MATLAB 2014a can be found here. Chapter V discusses the results and the calculation procedure used to obtain them. The inferences and conclusions are summarized in Chapter VI, whereas Chapter VII highlights the future scope of this study. The MATLAB code used can be found in the Appendix i along with a brief explanation of the code procedure. The

Appendix ii deals with the earlier iterations of the experiment which, even though they were insufficient to establish the desired results, helped in drawing some key conclusions.

A list of figures and tables precedes the thesis Chapters and a list of references can be found after the Chapters.

Chapter II

Literature Review

Vortex Generators:

A vortex generator[1] (VG) is an aerodynamic device, consisting of a small vane usually attached to a lifting surface (or airfoil, such as an aircraft wing) or a rotor blade of a wind turbine. VGs may also be attached to some part of an aerodynamic vehicle such as an aircraft fuselage or a car. When the airfoil or the body is in motion relative to the air, the VG creates a vortex, which, by removing some part of the slow-moving boundary layer in contact with the airfoil surface, delays local flow separation and aerodynamic stalling, thereby improving the effectiveness of wings and control surfaces, such as flaps, elevators, ailerons, and rudders. On both aircraft and wind turbine blades they are usually installed quite close to the leading edge of the airfoil in order to maintain steady airflow over the control surfaces at the trailing edge. VGs are typically rectangular or triangular, about as tall as the local boundary layer, and run in span-wise lines usually near the thickest part of the wing. They can be seen on the wings and vertical tails of many airliners.

Vortex generators are positioned obliquely so that they have an angle of attack with respect to the local airflow in order to create a tip vortex which draws energetic, rapidly moving outside air into the slow-moving boundary layer in contact with the surface. A turbulent boundary layer is less likely to separate than a laminar one, and is therefore desirable to ensure effectiveness of trailing-edge control surfaces. Vortex generators are used to trigger this transition.

Factors influencing vortex strength

The literature review revealed the following influencing factors:

- Height-to-length ratio: In this thesis case, the chord length was fixed and the height was varied during the iterations. The height-to-length ratio is the most influencing factor in the study of vortex generators.

- Yaw angle/position of vortex generators: In this thesis, iterations 1 & 2 had a yaw angle of -5 degrees to wind flow. The iteration 3 had a yaw angle of -20 degrees to wind flow resulting in a stronger disrupted signal.
- Shape of the VGs: The past literature has considered rectangular, triangular, ramp type etc. VGs and had found that the triangular and rectangular VGs work the best under specific conditions. Theoretical models include the one by Smith[2] and a model presented by Velte et al.[3] that were developed and applied to show the helical symmetry of the vortices generated by a passive rectangular vane-type vortex generator. For several flow control applications, conventional VGs first introduced by Taylor[4] have been successfully applied onto aircraft wings for flow control that enhance mixing of the boundary layer and thus transferring high momentum fluid closer to the wall, thereby suppressing or delaying separation, as reported by Schubauer.[5] Furthermore, the experimental work carried out by Velte and the corresponding simulations made by Ferńandez-G´amiz et al.[6] showed that the primary vortex produced by a rectangular VG mounted on a flat plate achieves self-similarity for both axial and azimuthal velocities. The current VGs (trapezoidal) being considered here are a combination of both triangular and rectangular VGs.
- Co-rotating and Counter rotating VGs[7]: This thesis deals with co-rotating VGs.

Correlated results from the literature review conducted:

1. Research on Aerodynamic Drag Reduction by Vortex Generators[8] by Masaru KOIKE, Tsunehisa NAGAYOSHI and Naoki HAMAMOTO

An experimental study to identify the effect of VGs fitted on the roof of a car when the size and shape of the VGs is modified. Fig 2.1 shows the change in drag and lift coefficients as the VG height changes. The change in coefficient is seen to be decreasing as the VG height increases (left hand side graphs)

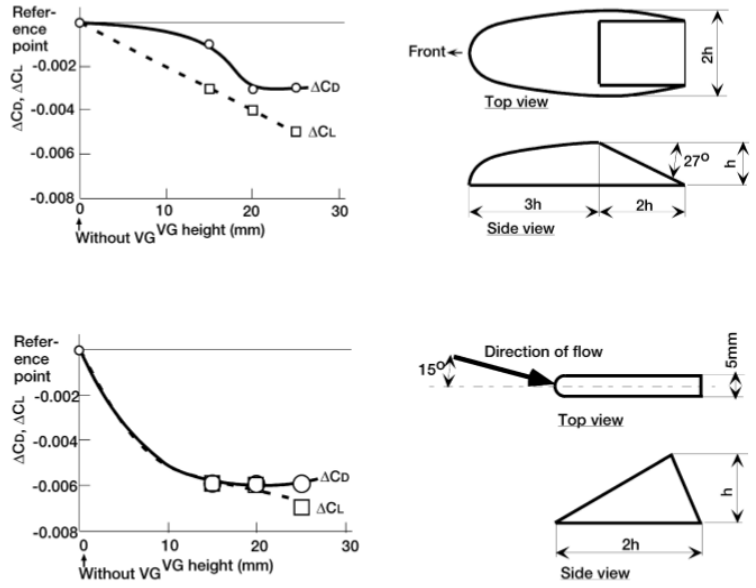

Fig 2.1: Effects of delta and ramp type VGs

For delta shaped VGs, Length/height = 2, Height = 15 mm, 20 mm and 25 mm (three types) Thickness = 5 mm

For ramp type VGs, Length/height = 2, Yaw angle = 15˚, Interval/height = 6

Results:

- The optimum height of the VGs is almost equivalent to the thickness of the boundary layer.
- Better effects are obtained from delta-wing-shaped VGs than from bump-shaped VGs.

2. Optimized vortex generators in the flow separation control around a NACA 0015 profile by H. Tebbiche, M.S. Boutoudj.[9]

The experiments were performed in order to determine the optimum VGs when they were placed at 10% chord length from the leading edge on the suction face of a NACA 0015 airfoil to improve the lift and drag coefficients. The aerodynamic measurements were accomplished in wind tunnel for several Reynolds numbers. The obtained results are analyzed according to several parameters such as the VG height, the aperture, the space between the same VG pair and the additional factor. δ represents the boundary layer thickness.

l : Vortex generators length,
b : Distance between two passive devices,
a : Space between the same VG,
h : Vortex generator height,
c : Vortex generator additional element,
β : Vortex generator aperture angle.

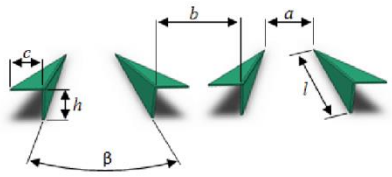

Figure 4. Passive VGs parameters

Table 2. Variation level on each factor.

Code	Factor	Level 1	Level 2	Units
A	a/δ	0.55	0.70	-
B	c/δ	0.30	0.45	-
C	h/δ	0.35	0.55	-
D	β	30	48	(°)

Fig 2.2: Varying the VG parameters

Results:

- The obtained results highlighted the importance of the C-factor represented by the vortex generators height which is the most influential factor with a contribution ratio of 22%.
- The optimized VGs geometry showed an improvement of 14% relative lift and 16% of drag reduction. The Reynolds number effect was determined and it shows that the flow at high velocity is more effective in increasing the Lift/Drag ratio.
- Comparative efficiency of the studied VGs highlighted a significant improvement on the flow control when the vortex generators are equipped with factor B.

3. Experimental Study on the Wake Characteristics of Vane-Type Vortex Generators in a Flat Plate Turbulent Boundary Layer[10]

Experimental study using stereoscopic-PIV on the wake characteristics of vortex generators over a flat plate turbulent boundary layer was carried out. The triangular, trapezoidal, and rectangular generators of two different lengths at three angles of attack were tested.

Results:

- The tendency of peak vorticity generation in the near wake region for each generator configuration was very sensitive to angle of attack and length of the generator. When l/h = 5, the peak vorticity in the near wake of the rectangular generator was largest only at $\alpha = 10°$, and when l/h = 2, it was largest at all angles of attack. When $\alpha = 20°$, for the case of l/h = 5, the triangular generator produced the largest vorticity.
- The vorticity decay characteristics with downstream distance also depend strongly on the generator shape and angle of attack. This signifies that the initial peak vorticity strength in the near wake does not imply its strength tendency at further downstream stations.
- The vortex of the triangular generator was formed at lower position than those of the trapezoidal and rectangular generators.

4. Computational study of the vortex path variation with the VG height by U. Fern´andez-G´amiz, G. Zamorano and E. Zulueta[11]

An experimental study of the variation of the path and the development of the primary vortex generated by a rectangular VG mounted on a flat plate with five different heights $h = \delta$, $h_1 = 0.8\delta$, $h_2 = 0.6\delta$, $h_3 = 0.4\delta$ and $h_4 = 0.2\delta$, where δ is the local boundary layer thickness.

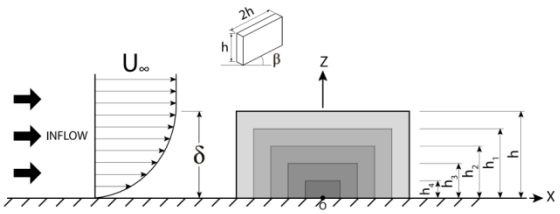

Figure 1. VG dimensions.

Table 1. VG heights and Drag coefficients.

VG	% of δ	Height (m)	C_D	$\Delta C_D(\%)$
h	100	0.25	0.1786	100
h_1	80	0.20	0.1585	88
h_2	60	0.15	0.1340	75
h_3	40	0.10	0.1054	59
h_4	20	0.05	0.0796	44

Fig 2.3: Effect of varying VG height

Results:

- The VG scaling significantly affects the vortex trajectory and the peak vorticity generated by the primary vortex.
- The peak vorticity decays exponentially and inversely proportional to x/δ. As expected, the magnitude of the peak vorticity decreases as the height of the VG is reduced.
- Of the five types of VG studied, h, h_1, h_2, h_3 and h_4, the last one was the most effective in terms of producing non-dimensional positive circulation just downstream of the device at the stream-wise station of 5δ

Parameter Varied	Expected Results
1) Height	Vortex formation moves away with increased height
2) Vortex Trapezoidal Angle (Front side)	Exact results not known from the papers read. Expected results: a) Vortex strength would increase/decrease b) Vortex location would move

Table 2.1: VG parameter varied in the study

Pressure Coefficient:

The pressure coefficient[12] *(C_p)* is a dimensionless number which describes the relative pressures throughout a flow field in fluid dynamics. The pressure coefficient is used in aerodynamics and hydrodynamics. Every point in a fluid flow field has its own unique pressure coefficient, *Cp*. The pressure coefficient can be calculated as

$$C_p = \frac{p - p_\infty}{\frac{1}{2}\rho V_\infty^2}$$

Where:

C_p = Coefficient of Pressure

p = pressure at ports

p_∞ = ambient pressure

ρ = air density (kg/m^3)

V_∞ = Wind Velocity

This relationship is valid for the flow of incompressible fluids where variations in speed and pressure are sufficiently small that variations in fluid density can be neglected. This is a reasonable assumption when the Mach Number is less than about 0.3.

- *Cp* of zero indicates the pressure is the same as the free stream pressure
- *Cp* of one corresponds to the stagnation pressure and indicates a stagnation point
- Fluctuations in values of *Cp* indicate the pressure variation in the flow

In the fluid flow field around a body there will be points having positive pressure coefficients up to one, and negative pressure coefficients including coefficients less than minus one, but nowhere will the coefficient exceed plus one because the highest pressure that can be achieved is the stagnation pressure.

Circulation:

In fluid dynamics, circulation[13] is the line integral around a closed curve of the velocity field. Circulation is normally denoted Γ (Greek uppercase gamma). If letter V is the fluid velocity on a small element of a defined curve, and dl is a vector representing the differential length of that small element, the contribution of that differential length to circulation is $d\Gamma$:

$$d\Gamma = \mathbf{V} \cdot \mathbf{dl} = |\mathbf{V}||d\mathbf{l}| \cos\theta$$

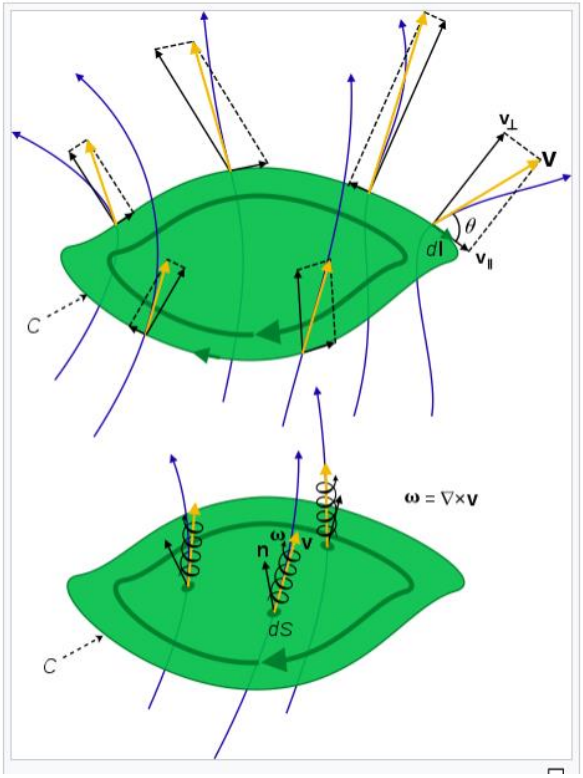

Fig 2.4: Circulation in flow

Where, θ is the angle between the vectors V and dl.

The circulation around a closed curve C is the line integral

$$\Gamma = \oint_C \mathbf{V} \cdot d\mathbf{l}$$

The dimensions of circulation are length squared, divided by time; $L^2 \cdot T^{-1}$, which is equivalent to velocity times length.

In the above diagram (Fig. 2.4), the parameters shown are field lines of a velocity field *v*, around the boundary of an open curved surface with infinitesimal line element dl along boundary, and through its interior with *dS* the infinitesimal surface element and n the unit normal to the surface. Top: Circulation is the line integral of v around a closed loop C. Project *v* along *dl*, then sum. Here v is split into components perpendicular (⊥) parallel (∥) to dl, the parallel components are tangential to the closed loop and contribute to circulation, the perpendicular components do not. Bottom: Circulation is also the flux of vorticity ω through the surface, and the curl of v is heuristically depicted as a helical arrow (not a literal representation). Note the projection of v along dl and curl of v may be in the negative sense, reducing the circulation.

Vorticity:

In continuum mechanics, the vorticity[14] is a pseudovector field that describes the local spinning motion of a continuum near some point (the tendency of something to rotate), as would be seen by an observer located at that point and traveling along with the flow. Conceptually, vorticity could be determined by marking the part of continuum in a small neighborhood of the point in question, and watching their relative displacements as they move along the flow. The vorticity vector would be twice the mean angular velocity vector of those particles relative to their center of mass, oriented according to the right-hand rule. This quantity must not be confused with the angular velocity of the particles relative to some other point.

More precisely, the vorticity is a pseudovector field **ω**, defined as the curl (rotational) of the flow velocity ***v*** vector. The definition can be expressed by a vector analysis formula. Mathematically, the vorticity of a three-dimensional flow is a pseudovector field, usually denoted by **ω**, defined as the curl or rotational of the velocity field ***v*** describing the continuum motion. In Cartesian coordinates:

$$\vec{\omega} = \nabla \times \vec{v} = \left(\frac{\partial}{\partial x}, \frac{\partial}{\partial y}, \frac{\partial}{\partial z}\right) \times (v_x, v_y, v_z)$$
$$= \left(\frac{\partial v_z}{\partial y} - \frac{\partial v_y}{\partial z}, \frac{\partial v_x}{\partial z} - \frac{\partial v_z}{\partial x}, \frac{\partial v_y}{\partial x} - \frac{\partial v_x}{\partial y}\right)$$

In words, the vorticity tells how the velocity vector changes when one moves by an infinitesimal distance in a direction perpendicular to it.

In a two-dimensional flow where the velocity is independent of the z coordinate and has no ***z*** component, the vorticity vector is always parallel to the z axis, and therefore can be expressed as a scalar field multiplied by a constant unit vector ***z***:

$$\vec{\omega} = \nabla \times \vec{v} = \left(\frac{\partial}{\partial x}, \frac{\partial}{\partial y}, \frac{\partial}{\partial z}\right) \times (v_x, v_y, 0) = \left(\frac{\partial v_y}{\partial x} - \frac{\partial v_x}{\partial y}\right) \vec{z}$$

Where ∇ is the del operator. The vorticity of a two-dimensional flow is always perpendicular to the plane of the flow, and therefore can be considered a scalar field.

The vorticity is related to the flow's circulation (line integral of the velocity) along a closed path by the (classical) Stokes' theorem[14], namely, for any infinitesimal surface element C with normal direction $\vec{n}$ and area *dA*, the circulation *dΓ* along the perimeter of *C* is the dot product $\vec{\omega} \cdot (dA\vec{n})$ where ω is the vorticity at the center of C.

The definitions of circulation a and vorticity and the relationship between circulation and vorticity give two key equations used to calculate the results in this document

1. The mean tangential velocity at the radius of the area dA would be: $V = \Gamma / (2\pi r)$
2. For a finite area, the average normal component of vorticity is given by the circulation divided by the area, which is considered in this thesis

Chapter III

Experimental setup:

The experimental setup consisted of 3 main components:

1) Wind Tunnel
2) Pressure sensing equipment
3) Flat Plate with Vortex Generator/s

The experiment was setup at the wind tunnels on campus – the Low speed Wind Tunnel (LWT) and the Kirsten Wind Tunnel (KWT). The first iteration (Appendix ii) was conducted in the LWT and it was discovered that the sensing equipment in the Tunnel were not appropriate for the desired results. The second iteration (Appendix ii) was conducted using the flat plate from first iteration and the sensing equipment from the KWT. The results obtained were improved and two conclusions could be drawn:

a) The type of vortex generator to be used for the third iteration (height = 1 inch angle = 55 degrees)
b) The yaw angle of mounting the vortex generator with respect to wind flow should be approximately 20 degrees

This information was used to carry out iteration 3 which is described in this document.

Wind Tunnel:

The Kirsten Wind Tunnel (KWT)[15] is a subsonic, closed circuit, double return wind tunnel (Fig 3.1). The tunnel has a test section with a rectangular 8’ x 12’ cross-section that is 10 feet long. Two sets of 14’ 9”-diameter seven-bladed propellers move the air up to 200 MPH through the test section. A computer-automated model positioning and data acquisition system ensures testing efficiency and precise measurements while a networked data reduction and plotting system allows for immediate data visibility. Most tests make use of KWT’s six-component external balance.

Tunnel Characteristics

Air Speeds	5-200 MPH (90 m/s, 295 ft/s)
Dynamic Pressures	0.07-100 psf
Flow Angularity	Upflow = -0.012°, Crossflow = 0.0°
Turbulence Intensity	0.72%
Test Section	8’ tall, 12’ wide, 10’ long (2.44x3.66x3.05m)
External Balance Limits	Lift: ±2500 lbs ±11120 N Drag: ±250 lbs ±1112 N Side: ±250 lbs ±1112 N Pitching: ±5000 in-lbs ±564.9 N-m Yawing: ±5000 in-lbs ±564.9 N-m Rolling: ±5000 in-lbs ±564.9 N-m
Model Positioning	Fully automated pitch and yaw accurate to ±0.02°
Data Reduction	Semi-corrected plots of data available in real-time. A separate data set with final corrections is produced as appropriate with customer input.
Flow Visualization	Smoke, oils, china clay, sublimation, UV minitufts
Electronic Pressure Scanning	Scanivalve EPS Modules: one 64-Port Dual Bank Module (±0.007psi) and one 32-Port Single Bank Module (±0.005psi)
Test Object Types	Scale-model Aircraft, Scale-model Ground Vehicles, UAV’s, Bicycles, Motorcycles, Racing Yacht Keels

Table 3.1: Kirsten wind tunnel capabilities

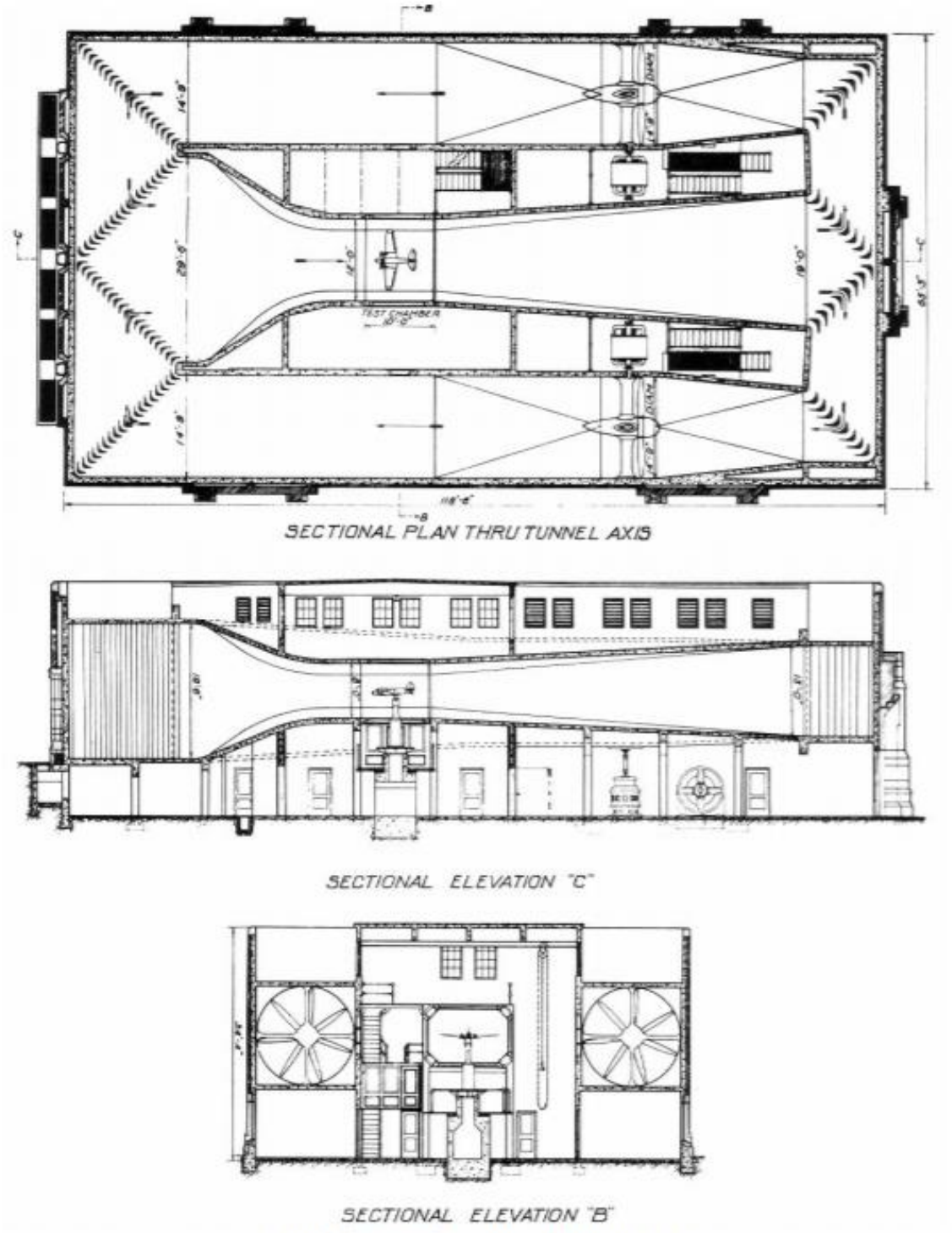

Figure 1: 3-View of Kirsten Wind Tunnel Building

Fig 3.1: KWT Layout

The test section (Fig 3.2) is vented to the atmosphere by two vents (5 feet long, 2 inches wide) located on the walls at the trailing edge of the test section. The vents keep the test section static pressure equal to approximately atmospheric pressure.

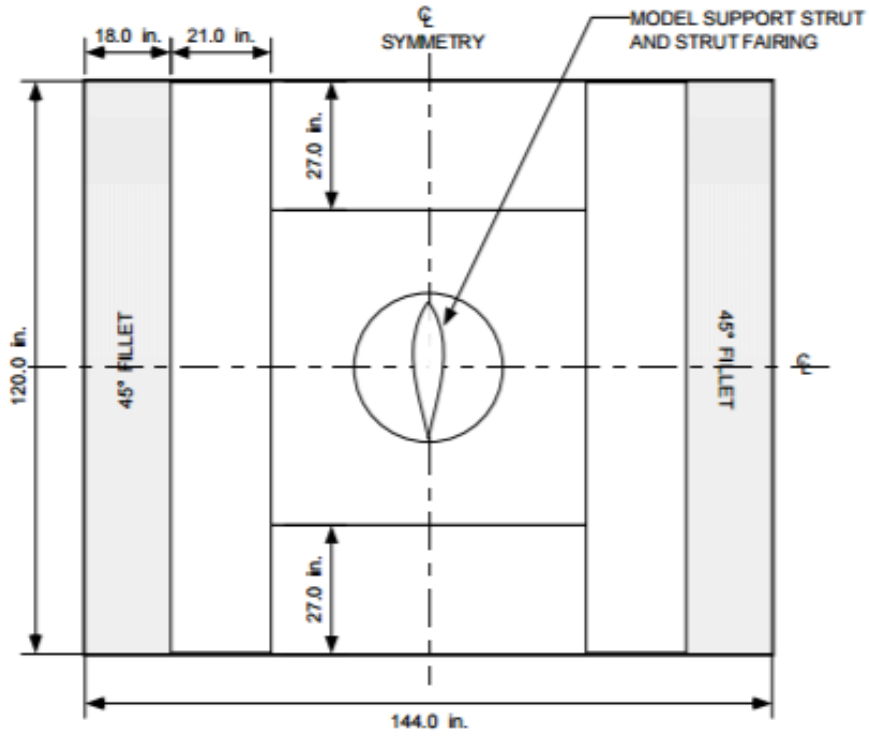

Fig 3.2 Tunnel Test Section

Test Section Instrumentation:

1) Dynamic Pressure Transducer: The dynamic pressure in the test section is measured by a precision differential pressure transducer: Mensor model DPG II 1500. It has a full-scale range of ±0.75 psi, with an accuracy of ±0.01% of full scale. The transducer is calibrated every six months using a primary standard traceable to the National Institute of Standards & Technology (NIST).
2) Test Section Static Pressure Transducer: The static pressure in the test section is measured by an absolute pressure transducer: Omega model PX425-030AV. It has a full-scale range of 0 to 30 psi with an accuracy of ±0.05 % of full scale.

3) Test Section Temperature: The test section static temperature is measured by a Resistive Temperature Device (RTD), manufactured by National Semiconductor. It has a full-scale range of 5 to 300 degree Fahrenheit with an accuracy of ± 1 degree Fahrenheit.

Pressure Sensing Equipment:

An electronic pressure scanning system (EPS) [16] is the primary means for acquiring pressure data. The UWAL Scanivalve[17] EPS module having 32-port, 0.72-psi range module, Model ZOC 23B (Fig 3.3) was used. The module has an accuracy of 0.05% of the full-scale range. The system can be automatically calibrated in five minutes. Calibrations need to be performed at least every hour to ensure the accuracy of the data. This system allows simultaneous recording of up to eight modules. Some characteristics of the ZOC 23B are:

- 0 - 50 psi pressure range
- Field-replaceable pressure sensors
- Patented micro-valves that make this miniature module possible (0.3 cu. in.)
- 20kHz scan rate
- Duplex 64 pressure inputs with 32 pressure sensors
- On-board sensor excitation regulator

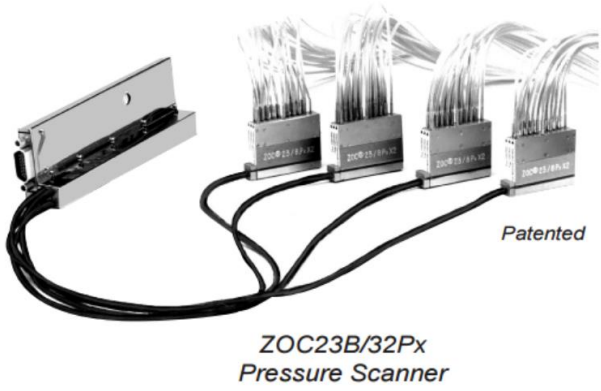

Fig 3.3: ZOC 23 pressure sensor

An integral "duplexing" valve is available to allow the ZOC23B's 32 sensors to service up to 64 input pressures. The integral calibration valve has four modes of operation: operate, calibrate, purge, and leak test; each activated by applying the appropriate pneumatic control pressure. This calibration valve allows the ZOC sensors to be automatically calibrated while on-line.

Specifications

Inputs (Px): 64 or 32 .042 inch (1.067mm) O.D. tubulations

Full Scale Ranges: ±10, 20 inch H_2O, 1, 2.5, 5, 15, 50 psid (±2.5, 5, 7, 17, 35,100, 350 kPa)

Accuracy:[1]

10 inch H_2O†	±0.25% F.S.
20 inch H_2O‡	±0.25% F.S.
1 to 2.5 psid	±0.15% F.S.
5 to 50 psid	±0.10% F.S.

Sensor Addressing: 5 bit binary, CMOS level

Full Scale Output: Standard: ±2.5Vdc Optional: ±5Vdc, ±10Vdc

Resolution: Infinite

Scan Rate: 20kHz

Temperature: 0° to 60°C

Temperature Sensitivity:

Range	Zero	Span
10 inch H_2O	0.25% FS/°C	0.1% FS/°C
20 inch H_2O	0.20% FS/°C	0.1% FS/°C
1 to 50 psid	0.10% FS/°C	0.1% FS/°C

Connector Type: Cannon 15 pin MDM 15SL2P

Power Requirements: ± 15Vdc @ 45mA

Overpressure Capability: (With no damage) 10 inch H_2O, 20 inch H_2O, 1 psid = 10 psi (70kPa) 2.5-50 psid = 400% or 75 psi (517kPa) (whichever is less)

Maximum Reference Pressure: 50 psig (345kPa)

Media Compatibility: Gases compatible with silicon, silicone, aluminum, and Buna-N

Weight: ZOC23B/32Px: 6.00 ozs. (170 gm) ZOC23B/32PxX2: 6.13 ozs. (174 gm) ZOC23B/8Px muxless: .93 ozs. (27 gm)

Ordering Information

ZOC23B/32Px - 1 psid

- Model
- Pressure Range
- Write "Valveless" here for this option only.

-32Px for 32 Inputs
-32PxX2 for 64 Inputs
-8Px for 8 Inputs Muxless
-8PxX2 for 16 Inputs Muxless

[1] Note: Accuracies are following a calibration with Scanivalve DSM or RAD data systems, in a thermally stable environment.

† 10 inch H_2O = 25.4 cm H_2O = .36127 psi

‡ 20 inch H_2O = 50.8 cm H_2O = .72254 psi

Fig 3.4: ZOC 23 Specifications

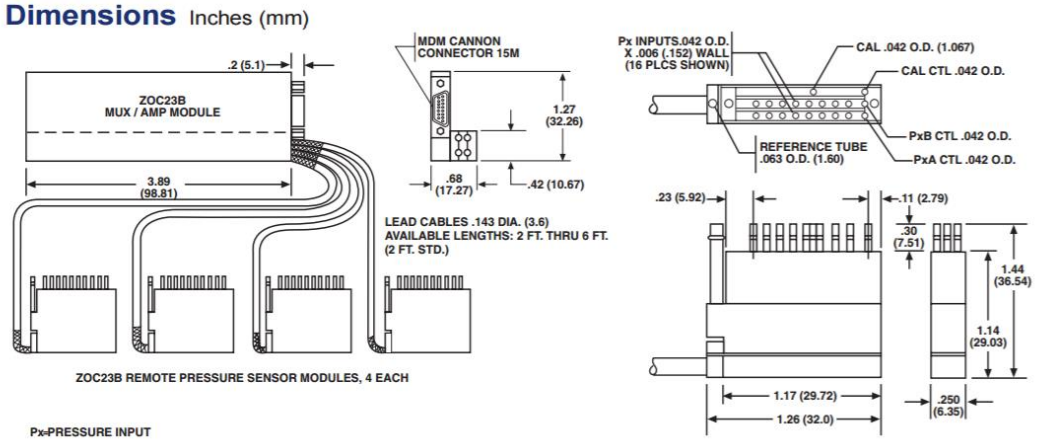

Fig 3.5: ZOC 23 Dimensions & Connection Diagram

The ZOC23B electronic pressure scanner is specifically designed for space-constrained use. The remote pressure sensor modules can be mounted in any position to fit where no other pressure scanners can be used. The small size makes it possible to locate the remote modules very close to the pressure orifices to maximize frequency response.

Flat Plate with Vortex Generators:

The iteration 3 of flat plate testing consisted of two flat plates as follows.

Plate 1: A 27 inch by 18 inch rectangular plate with 3 VGs angled at -20 degrees to the wind flow. Plate 1 had 63 pressure ports in a pattern of three columns of 21 ports each. The below figure (Fig 3.6) shows the plan view of the Plate 1.

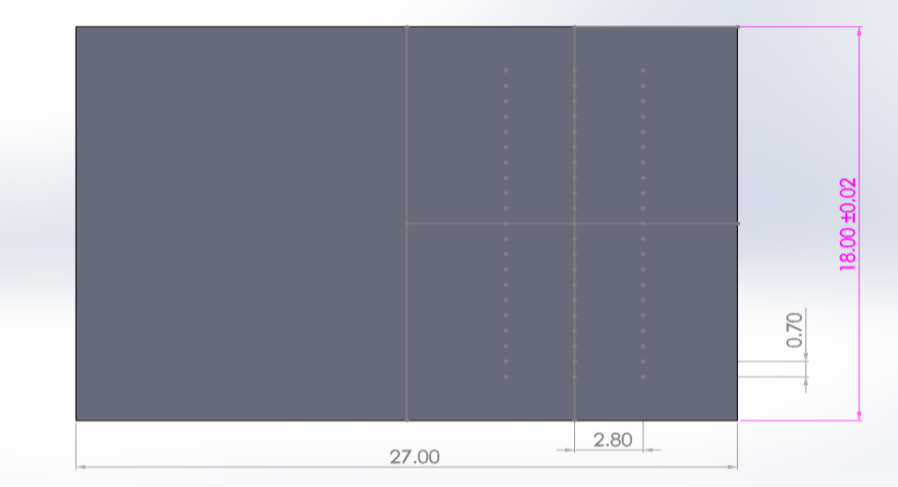

Fig 3.6: Solidworks model of Plate 1

Plate 2: A 30 inch by 9 inch plate with 1 VG angled at -20 degrees to the wind flow. Plate 2 had 63 ports as well with 21 columns of three ports each. The below figure (Fig 3.7) shows the plan view of the Plate 2.

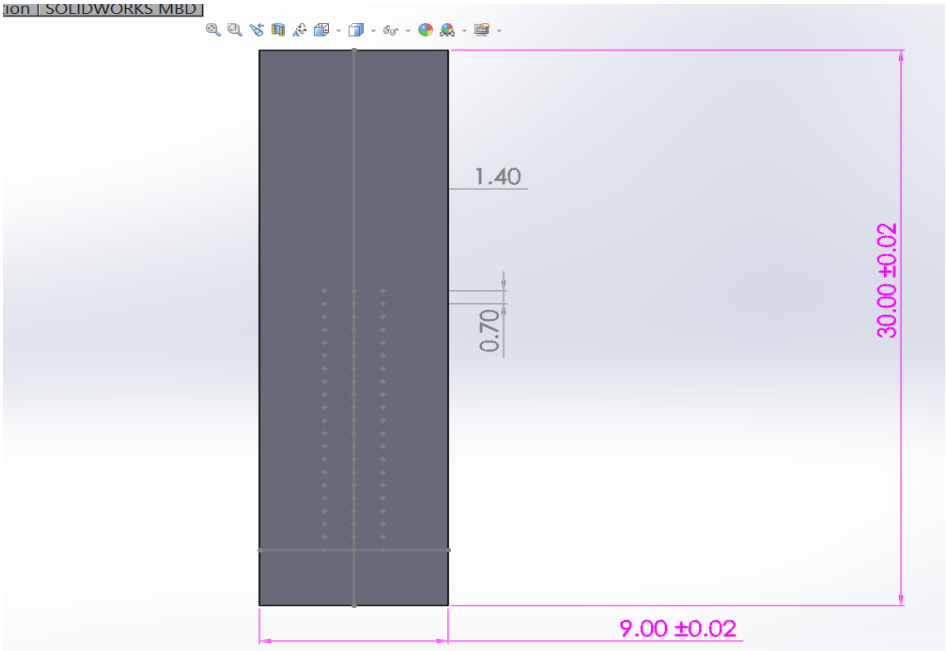

Fig 3.7: Solidworks model of Plate 2

Vortex Generators:

The Vortex Generators had the following dimensions:

Chord Length: c = 3.5 inch

Height: h = 1 inch

VG Angle of attack: β = 55 degrees

Mounting Angle on plate: α = - 20 degrees to wind flow direction

VG thickness: t = 3/16 inch

VG Material: Steel

These dimensions were finalized after the comparative results obtained from the iterations 1 and 2 where five different type of VGs were tested for the same flow conditions.

Fig 3.8 & Fig 3.9 shows the plates fitted with the VGs

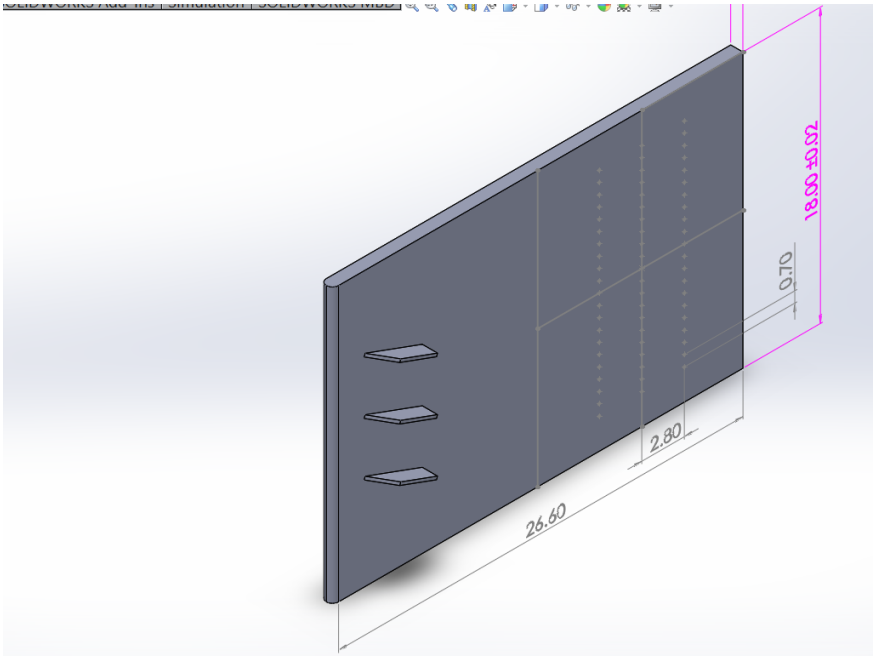

Fig 3.8: Plate 1 with 3 VGs

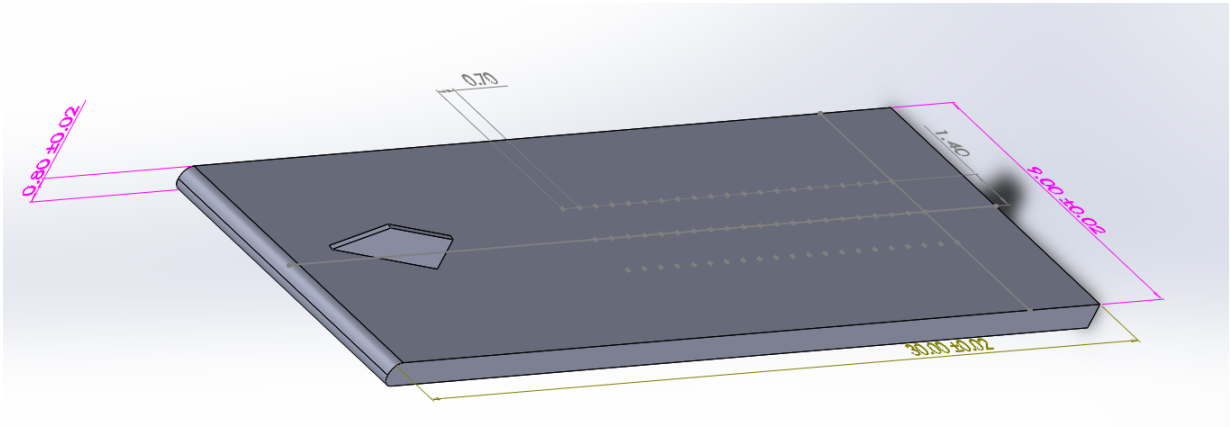

Fig 3.9: Plate 2 with 1 VG

Fig 3.10 & Fig 3.11 are representative of the plates fitted in the wind tunnel with the wind direction shown.

Wind Direction

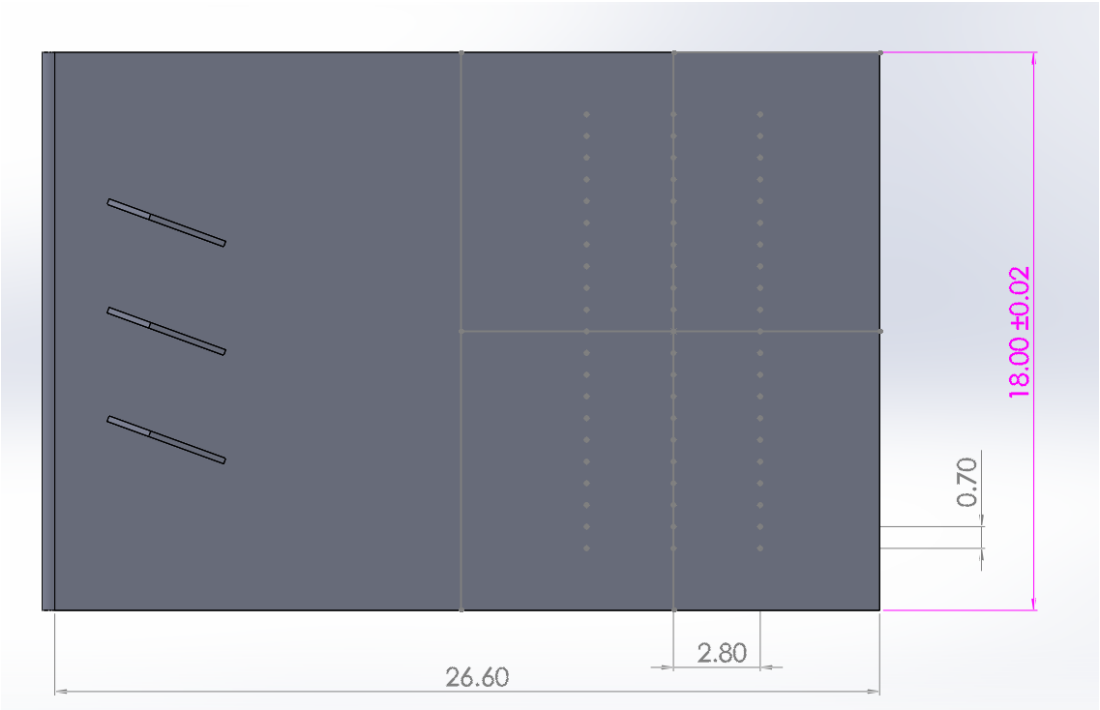

Fig 3.10: Plate 1 with 3 VGs angled -20 deg to the wind. 63 pressure ports in 3 columns of 21 each. Wind direction is shown.

Wind Direction

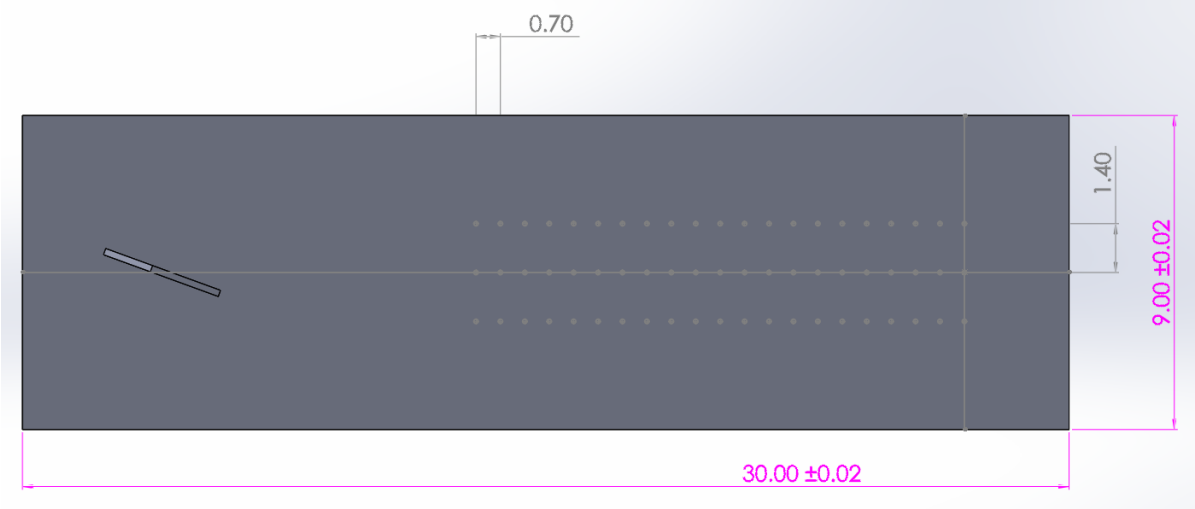

Fig 3.11: Plate 2: 1 VG angled -20 deg to wind with 63 pressure ports with 3 rows of 21 each. Wind direction is shown

Wind Tunnel Run Setup:

The EPS sensing equipment was connected to the plates and plates were mounted in the central mount in the KWT. Each Plate was tested for 2 tunnel runs; one with the VGs and one without. The data was recorded in the form of pressure coefficient (C_p) values in csv (comma separated variable) format which could then be accessed in MS Office – Excel. A typical tunnel run recorded the ambient pressure and temperature values (Fig 3.12). For Plate 1, the tunnel was run from speeds 0 to 80 mph with a data point recorded every 10 mph. For Plate 2, the tunnel was run from speeds 0 to 80 mph with a data point recorded every 10 mph (Fig 3.13). Each tunnel run took around 20 minutes including the initial calibration.

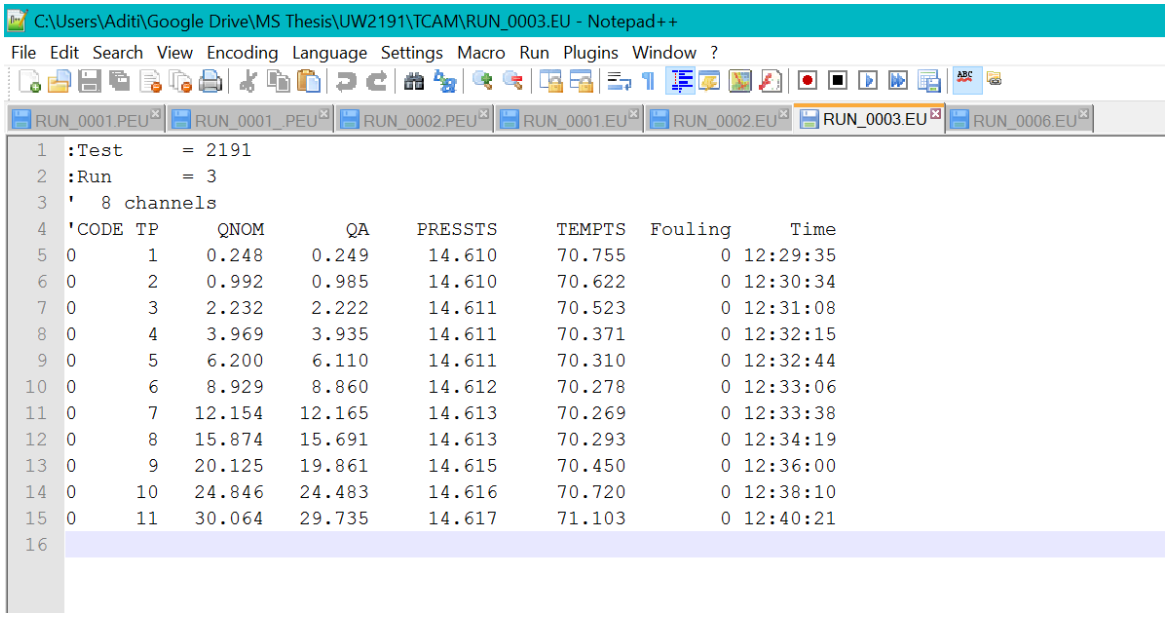


```
:Test      = 2191
:Run       = 3
'  8 channels
'CODE TP      QNOM       QA     PRESSTS     TEMPTS  Fouling     Time
0       1     0.248     0.249      14.610      70.755        0 12:29:35
0       2     0.992     0.985      14.610      70.622        0 12:30:34
0       3     2.232     2.222      14.611      70.523        0 12:31:08
0       4     3.969     3.935      14.611      70.371        0 12:32:15
0       5     6.200     6.110      14.611      70.310        0 12:32:44
0       6     8.929     8.860      14.612      70.278        0 12:33:06
0       7    12.154    12.165      14.613      70.269        0 12:33:38
0       8    15.874    15.691      14.613      70.293        0 12:34:19
0       9    20.125    19.861      14.615      70.450        0 12:36:00
0      10    24.846    24.483      14.616      70.720        0 12:38:10
0      11    30.064    29.735      14.617      71.103        0 12:40:21
```

Fig 3.12: Tunnel Run log showing the pressure and temperature measurement for each speed from 0 to 110 mph

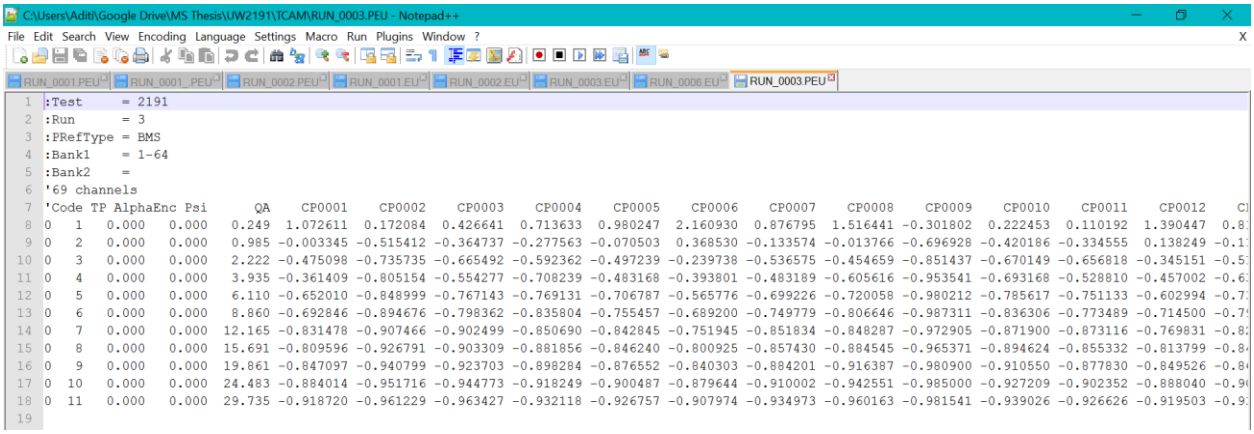

C:\Users\Aditi\Google Drive\MS Thesis\UW2191\TCAM\RUN_0003.PEU - Notepad++

File Edit Search View Encoding Language Settings Macro Run Plugins Window ?

RUN_0001.PEU | RUN_0001_.PEU | RUN_0002.PEU | RUN_0001.EU | RUN_0002.EU | RUN_0003.EU | RUN_0006.EU | RUN_0003.PEU

```
:Test     = 2191
:Run      = 3
:PRefType = BMS
:Bank1    = 1-64
:Bank2    =
'69 channels
'Code TP AlphaEnc Psi      QA     CP0001    CP0002    CP0003    CP0004    CP0005    CP0006    CP0007    CP0008    CP0009    CP0010    CP0011    CP0012    C
0   1   0.000   0.000   0.249  1.072611  0.172084  0.426641  0.713633  0.980247  2.160930  0.876795  1.516441 -0.301802  0.222453  0.110192  1.390447  0.8
0   2   0.000   0.000   0.985 -0.003345 -0.515412 -0.364737 -0.277563 -0.070503  0.368530 -0.133574 -0.013766 -0.696928 -0.420186 -0.334555  0.138249 -0.1
0   3   0.000   0.000   2.222 -0.475098 -0.735735 -0.665492 -0.592362 -0.497239 -0.239738 -0.536575 -0.454659 -0.851437 -0.670149 -0.656818 -0.345151 -0.5
0   4   0.000   0.000   3.935 -0.361409 -0.805154 -0.554277 -0.708239 -0.483168 -0.393801 -0.483189 -0.605616 -0.953541 -0.693168 -0.528810 -0.457002 -0.6
0   5   0.000   0.000   6.110 -0.652010 -0.848999 -0.767143 -0.769131 -0.706787 -0.565776 -0.699226 -0.720058 -0.980212 -0.785617 -0.751133 -0.602994 -0.7
0   6   0.000   0.000   8.860 -0.692846 -0.894676 -0.798362 -0.835804 -0.755457 -0.689200 -0.749779 -0.806646 -0.987311 -0.836306 -0.773489 -0.714500 -0.7
0   7   0.000   0.000  12.165 -0.831478 -0.907466 -0.902499 -0.850690 -0.842845 -0.751945 -0.851834 -0.848287 -0.972905 -0.871900 -0.873116 -0.769831 -0.8
0   8   0.000   0.000  15.691 -0.809596 -0.926791 -0.903309 -0.881856 -0.846240 -0.800925 -0.857430 -0.884545 -0.965371 -0.894624 -0.855332 -0.813799 -0.8
0   9   0.000   0.000  19.861 -0.847097 -0.940799 -0.923703 -0.898284 -0.876552 -0.840303 -0.884201 -0.916387 -0.980900 -0.910550 -0.877830 -0.849526 -0.8
0  10   0.000   0.000  24.483 -0.884014 -0.951716 -0.944773 -0.918249 -0.900487 -0.879644 -0.910002 -0.942551 -0.985000 -0.927209 -0.902352 -0.888040 -0.9
0  11   0.000   0.000  29.735 -0.918720 -0.961229 -0.963427 -0.932118 -0.926757 -0.907974 -0.934973 -0.960163 -0.981541 -0.939026 -0.926626 -0.919503 -0.9
```

Fig 3.13: Run log showing the C_p values at each of the 63 ports at speeds from 0 to 110 mph with data points at every 10 mph

Fig 3.14 to Fig 3.18 show the plates mounted in the tunnel with the pressure sensing equipment connected to the plates.

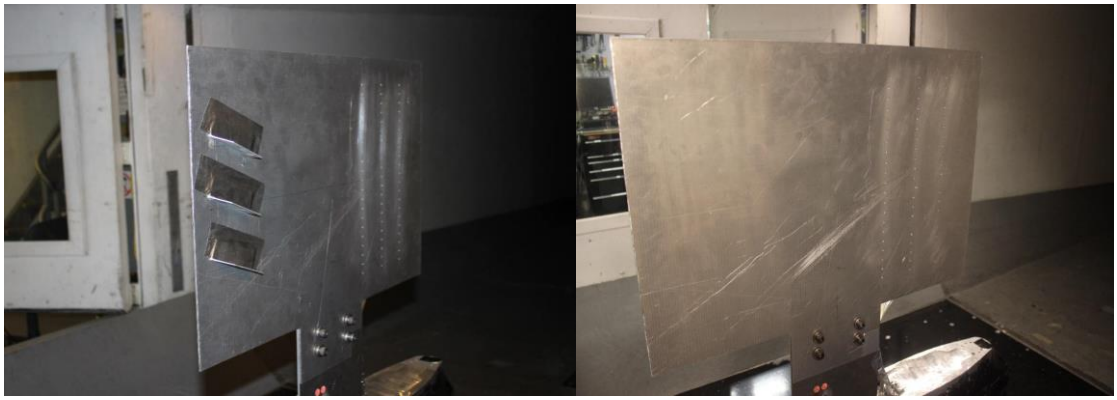

Fig 3.14: Plate 1 with (left image) & without (right image) VGs: Front view

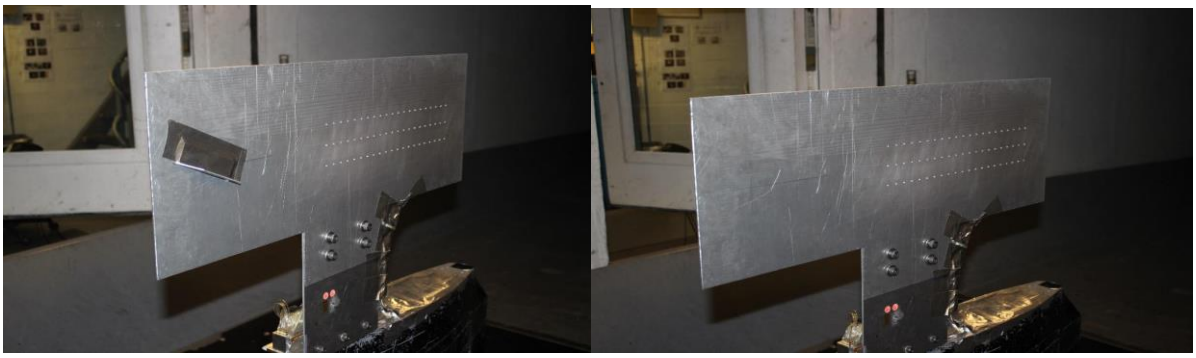

Fig 3.15: Plate 2 with (left image) & without (right image) VGs: Front view

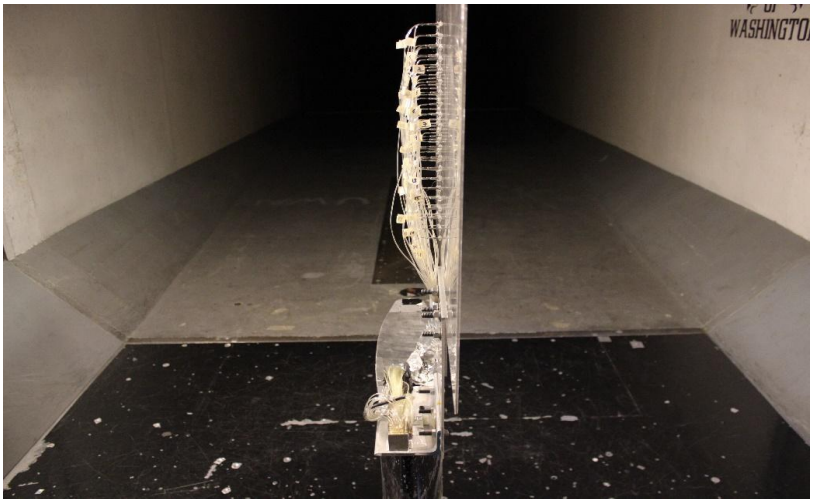

Fig 3.16: Plate mounting: view from Wind direction

Fig 3.17: Plate Mounting: pressure ports connected to the EPS. The sensing system is placed inside the tunnel mount

Fig 3.18: Plate1 & Plate 2: rear view

The tunnel was run from 0 to 80 mph for Plate 1 and 0 to 110 mph for Plate 2 with a data point taken at every 10 mph.

Chapter IV

Results

The tunnel run details are as follows:

Run No	Run Details	Speed Range for Run
Run 1	Plate 1 with no VGs	0 - 80 mph
Run 2	Plate 1 with 3 VGs, located as described in Chapter III	0 – 80 mph
Run 3	Plate 2 with 1 VG at center	0 – 110 mph
Run 4	Plate 2 with no VGs	0 – 110 mph

Table 4.1: Tunnel Run details

The maximum speeds that the plates could sustain without vibration were 80 mph for Plate 1 and 110 mph for Plate 2. For Plate 1, the 3 VGs are located between ports 5 & 7, 10 & 12 and 16 & 18 with the ports being located at every 0.7 inches span-wise.

Cp Plots:

The C_p values obtained from the tunnel were plotted using MATLAB 2014a. The following plots (Fig 4.1 and Fig 4.2) show the column-wise C_p variation in speed for Plate 1 with column 1 being the nearest to VGs and column 3 the farthest. Run 2 shows Plate 1 with 3 VGs. In Fig 4.1, there are two main dips, one at port 9 and the second at port 14. A lower *Cp* value as compared to the surrounding area could be indicative of a vortex. Similarly, in Fig 4.2, dips can be observed at ports 10 and 15.

The VGs affect the C_p creating the dips in the graph. The dips potentially indicate the low pressure areas corresponding to the possible vortex formation. Other alternative explanations could be general flow over the plate without vortices or possible edge effects from the plate.

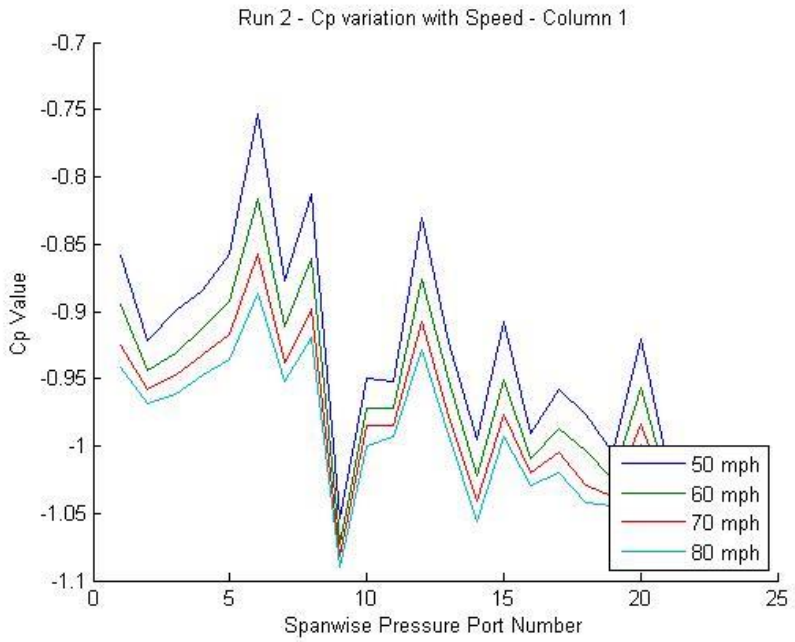

Fig 4.1: *Cp* variation for run 2 of Plate 1 for Column 1. The span wise ports are 0.7 inches apart from each other

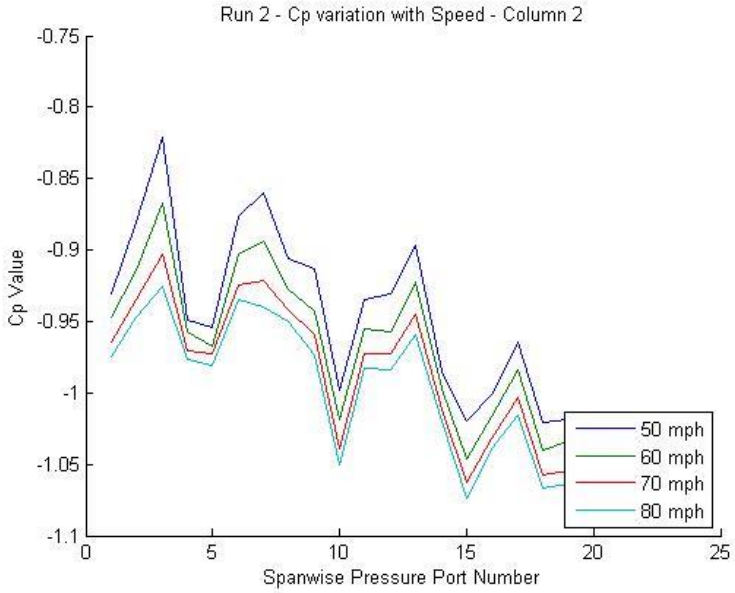

Fig 4.2: *Cp* variation for run 2 of Plate 1 for Column 2. The span wise ports are 0.7 inches apart from each other

Pressure Coefficient (*Cp*) Map

A better way to visualize the C_p variation is by using the MATLAB Contour Plot feature. The pressure coefficient values across all three column (in the case of Plate 1) and across all 3 rows (in the case of Plate 2) can be plotted together and relative to each other creating gradient contours across the plates.

The C_p variation for the different speeds is plotted for the Plate 1 for the Runs 1 and 2 and compared between the Runs. The development of the flow with respect to speed can thus be visualized. There are clear indications of low C_p value areas thus indicating the corresponding low pressure areas. The speeds compared here are 50 mph, 60 mph, 70 mph & 80 mph. The top 4 speeds were considered to study the flow development with increasing speeds.

A similar comparison has also been carried out for the Plate 2 where Run 3 represents the Plate with 1 VG and Run 4 represents Plate 2 without VGs. The speeds considered for comparison are 80 mph, 90 mph, 100 mph and 110 mph. The top 4 speeds were considered to study the flow development with increasing speeds.

The flow maps over plate surface can be superimposed on the plate in the following way (Fig 4.3 to 4.5) to show the location of the C_p and Velocity variations with respect to the pressure ports. The pressure ports can be seen in the Solidworks model and the MATLAB plots have been aligned to them. The figures also show the plate dimensions in inches. Each of the *Cp* and velocity maps can be superimposed in this way. The gradient alongside the plot shows the range of *Cp* or velocity values measured by the ports at the specific tunnel speed with blue representing the lower values and red representing the higher values.

Wind Direction ⟹

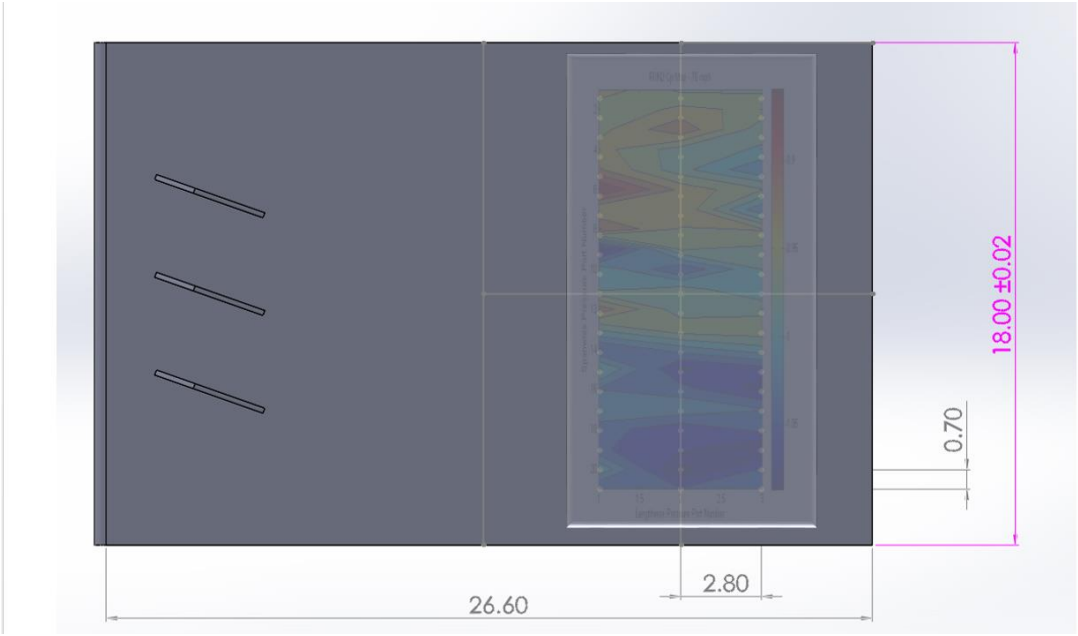

Fig 4.3: Plate 1: Superimposed *Cp* Map with transparency to show the pressure port locations

Wind Direction ⟹

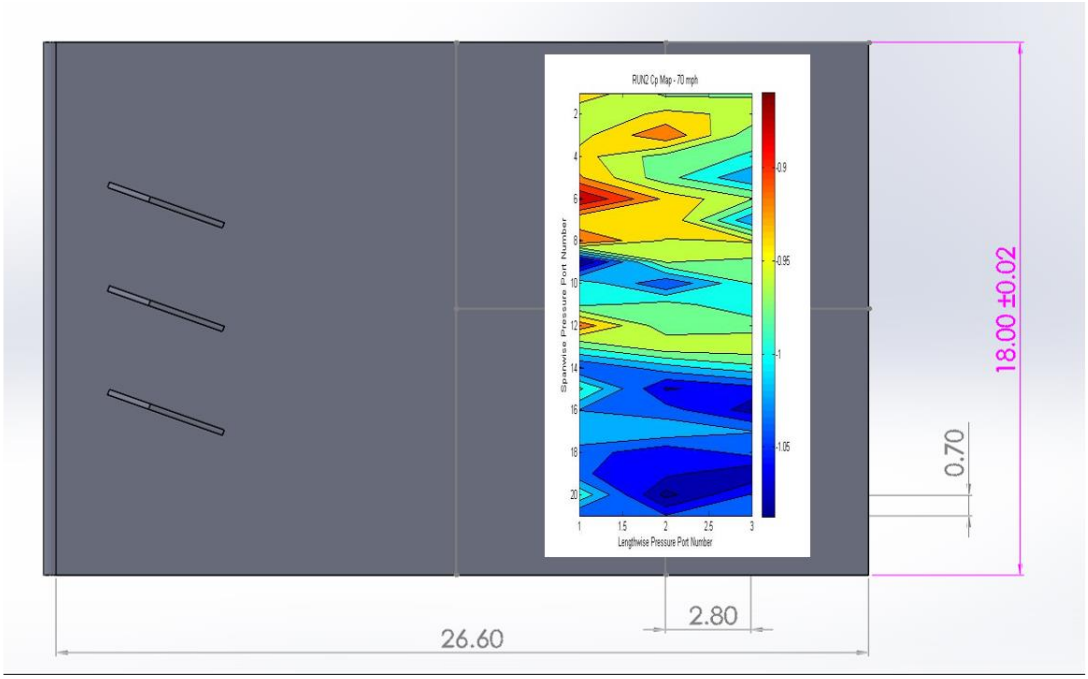

Fig 4.4: Plate 1: Superimposed *Cp* Map

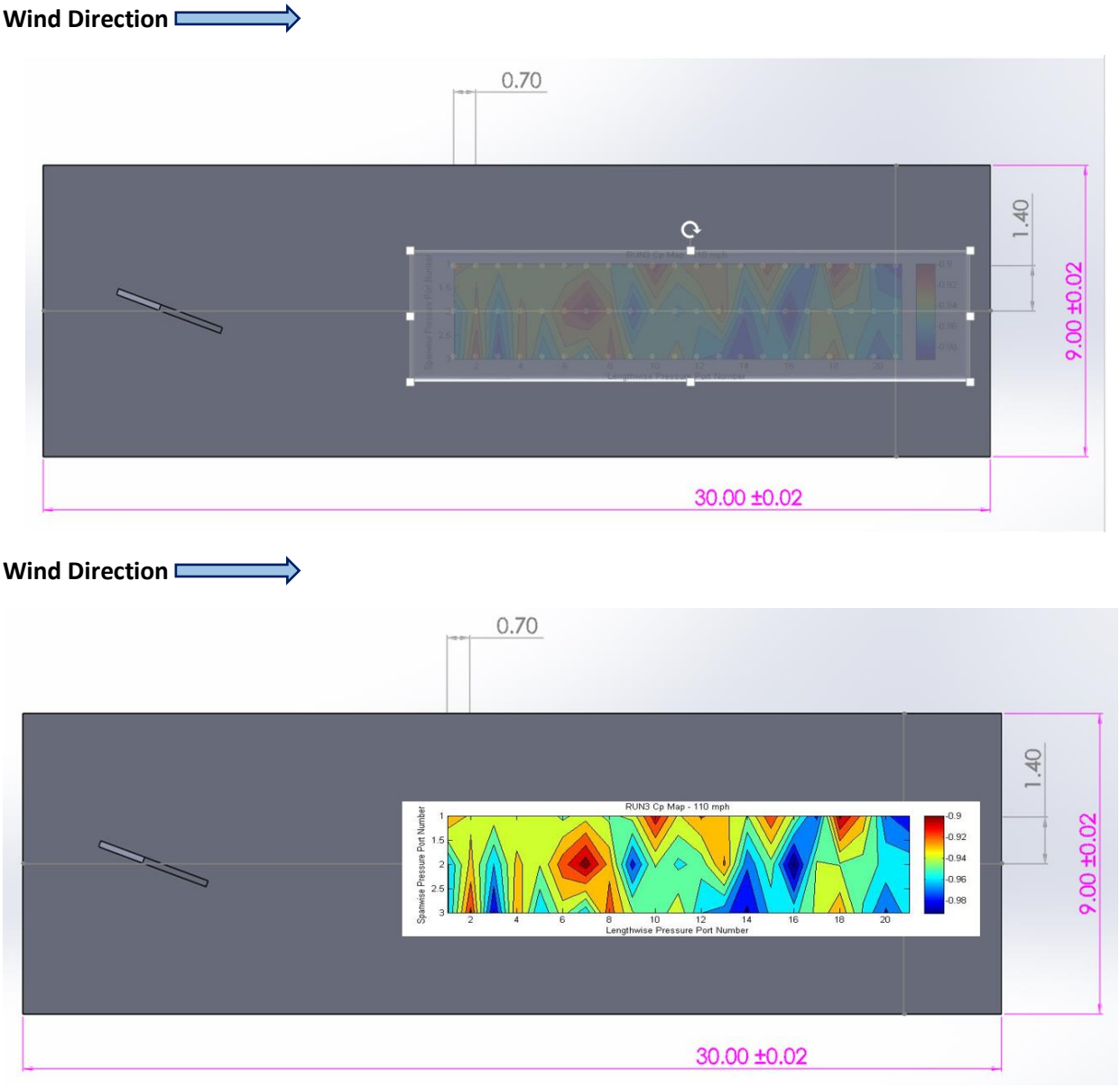

Fig 4.5: Plate 2: Superimposed *Cp* Map with transparency to show the pressure port locations and the superimposed *Cp* map

The *Cp* maps for individual speeds can be compared between runs 1 (Fig 4.6) & 2 (Fig 4.7) and between runs 4 (Fig 4.8) & 3 (Fig 4.9). The no VG runs (Runs 1 and 4) show lesser variation and closed contours as compared to runs with VGs (Runs 2 and 3).

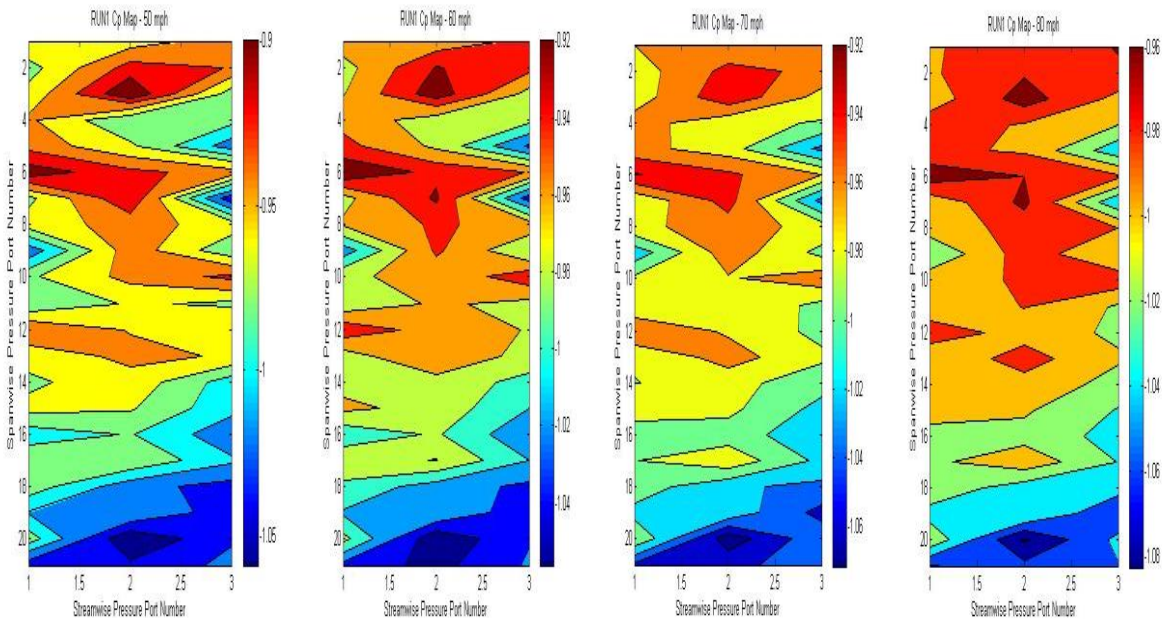

Fig 4.6: Plate 1 Run 1 *Cp* Maps for 50 mph, 60 mph, 70 mph and 80 mph. Spanwise ports are 0.7 inch apart and streamwise ports are 2.8 inches apart.

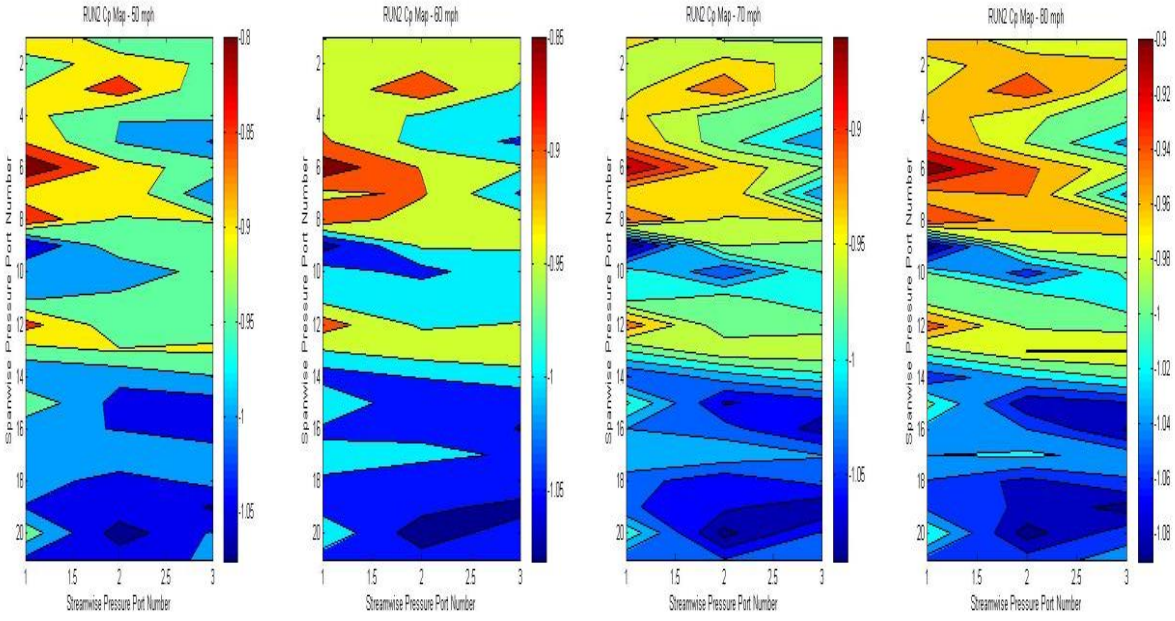

Fig 4.7: Plate 1 Run 2 *Cp* Maps for 50 mph, 60 mph, 70 mph and 80 mph. Spanwise ports are 0.7 inch apart and streamwise ports are 2.8 inches apart.

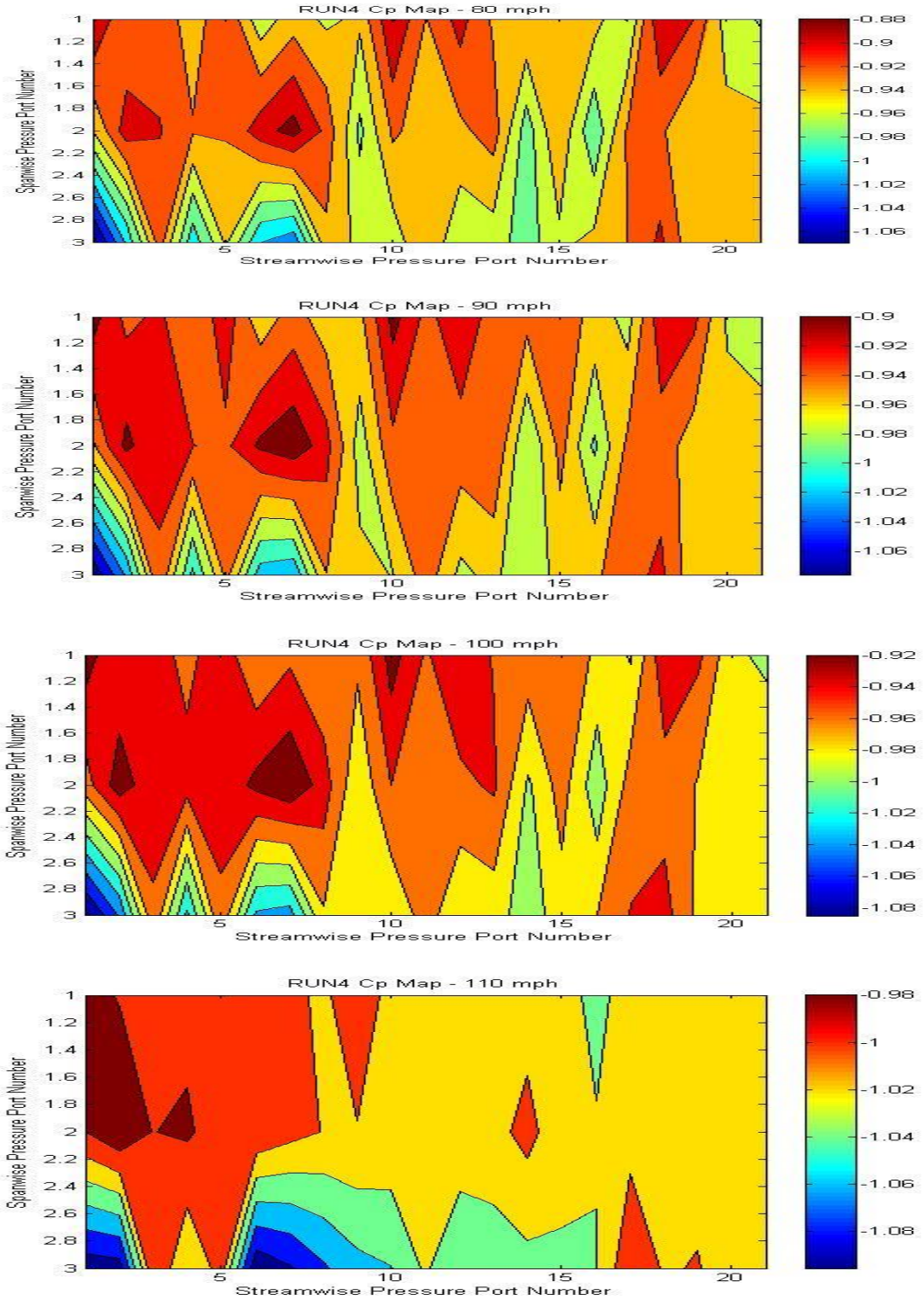

Fig 4.8: Plate 2 Run 4 *Cp* Maps for 80 mph, 90 mph, 100 mph and 110 mph. Spanwise ports are 1.4 inches apart and streamwise ports are 0.7 inches apart.

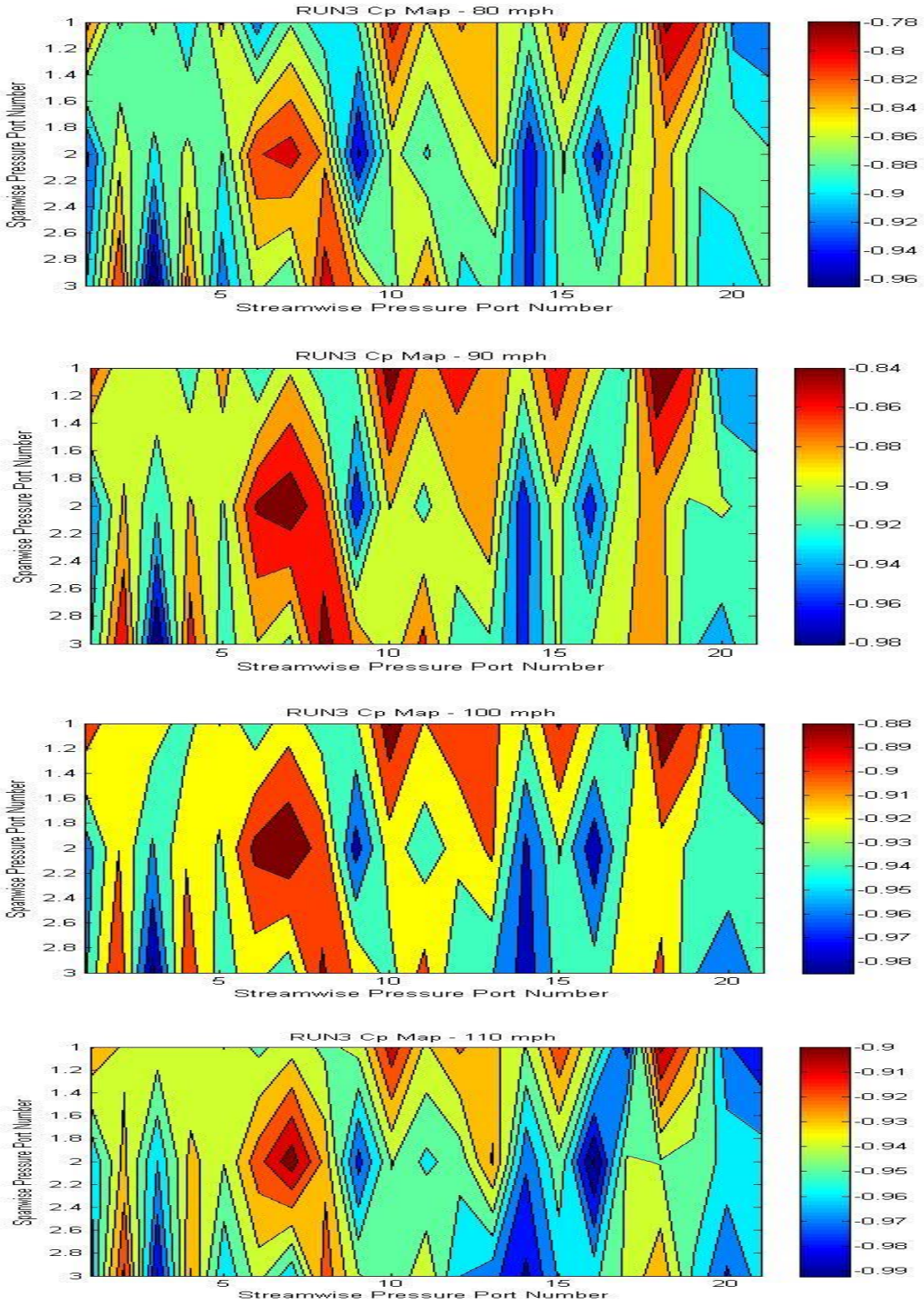

Fig 4.9: Plate 2 Run 4 *Cp* Maps for 80 mph, 90 mph, 100 mph and 110 mph. Spanwise ports are 1.4 inches apart and streamwise ports are 0.7 inches apart.

Velocity Maps:

The C_p values can also be used to calculate the velocity at each of the ports (refer formula in Chapter V). A velocity contour map can be created to show the velocity variation in the flow across the plates. Lower C_p values correspond to higher velocities. The comparative velocity maps for speeds 50 mph, 60 mph, 70, mph and 80 mph have been shown below for the Runs 1 (Fig 4.10) & 2 (Fig 4.11) for Plate 1 and the comparative velocity maps for the speeds 80 mph, 90 mph, 100 mph and 110 mph have been shown for the Runs 4 (Fig 4.12) & 3 (Fig 4.13) for Plate 2.

The presence of VGs in both the Plate cases influence the velocity field across the plate. The VG cases have higher velocity closed contour areas generated. These potentially indicate the presence of a vortex.

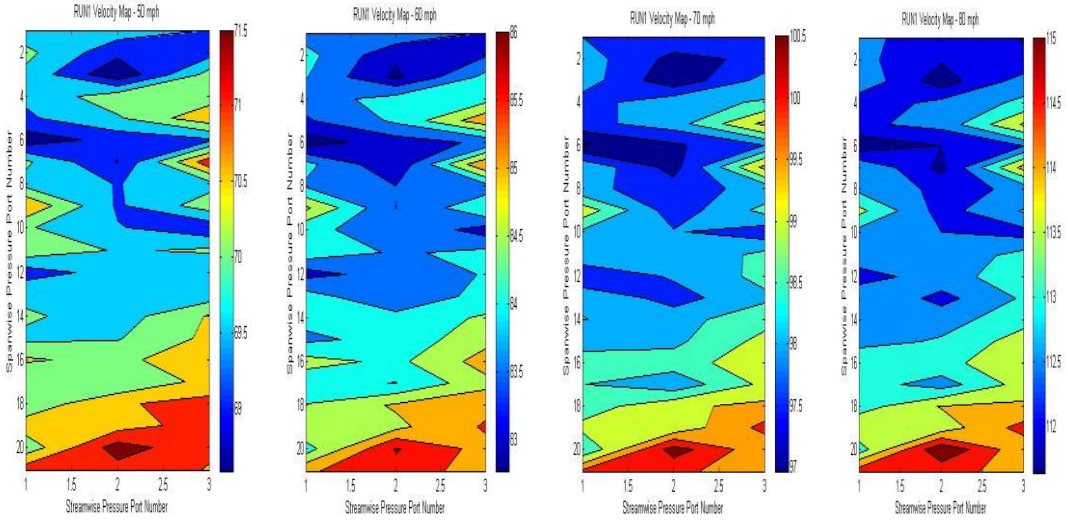

Fig 4.10: Plate 1 Run 1 Velocity Maps for 50 mph, 60 mph, 70 mph and 80 mph. Spanwise ports are 0.7 inches apart and streamwise ports are 2.8 inches apart.

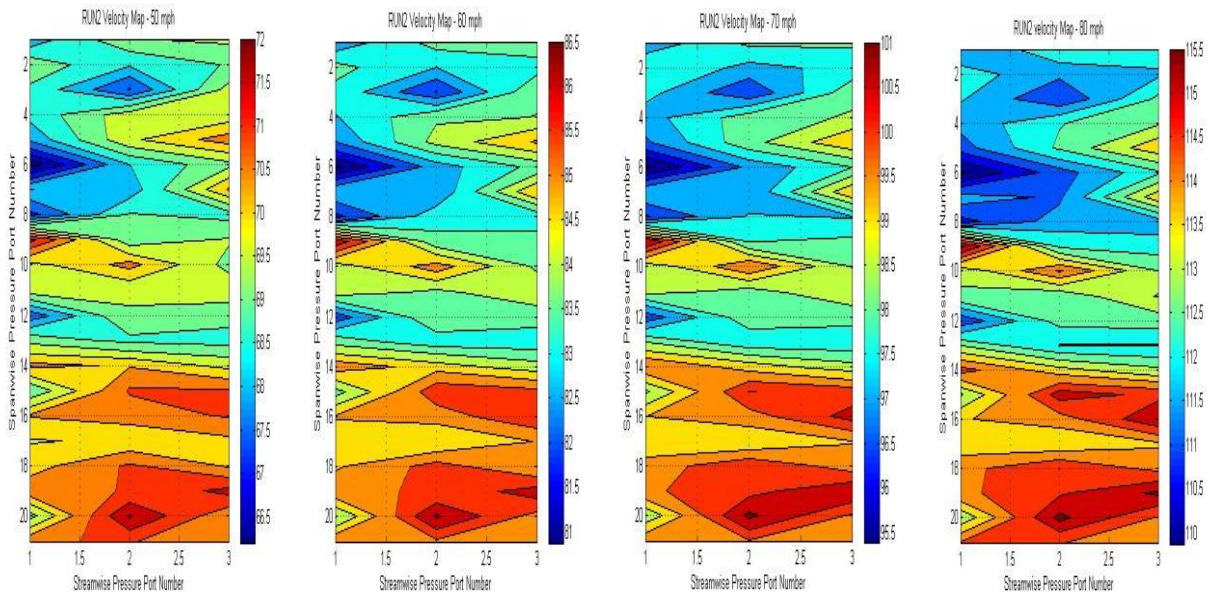

Fig 4.11: Plate 1 Run 2 Velocity Maps for 50 mph, 60 mph, 70 mph and 80 mph. Spanwise ports are 0.7 inches apart and streamwise ports are 2.8 inches apart.

A significant larger higher velocity area can be observed towards the lower end of the Plate 1 when the Run with VGs is conducted. This high velocity area also becomes darker red indicating comparatively higher velocities as compared to the surrounding region as the tunnel speed increases. This may indicate the vortices formed due to the VGs are contributing together to generate an overall high velocity area. This high velocity area can help predict the location of the vortex/vortices.

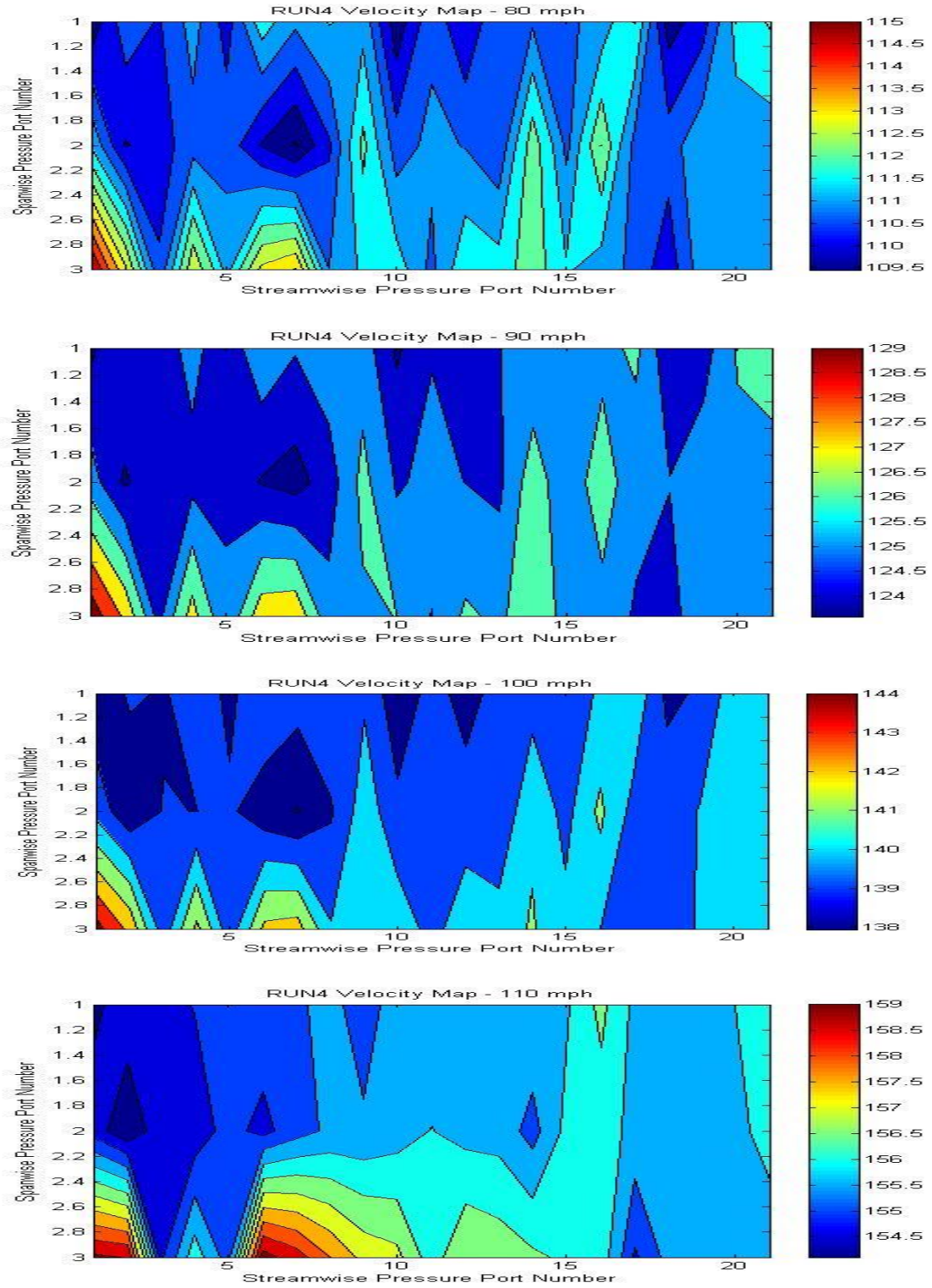

Fig 4.12: Plate 2 Run 4 Velocity Maps for 80 mph, 90 mph, 100 mph and 110 mph. Spanwise ports are 1.4 inches apart and streamwise ports are 0.7 inches apart.

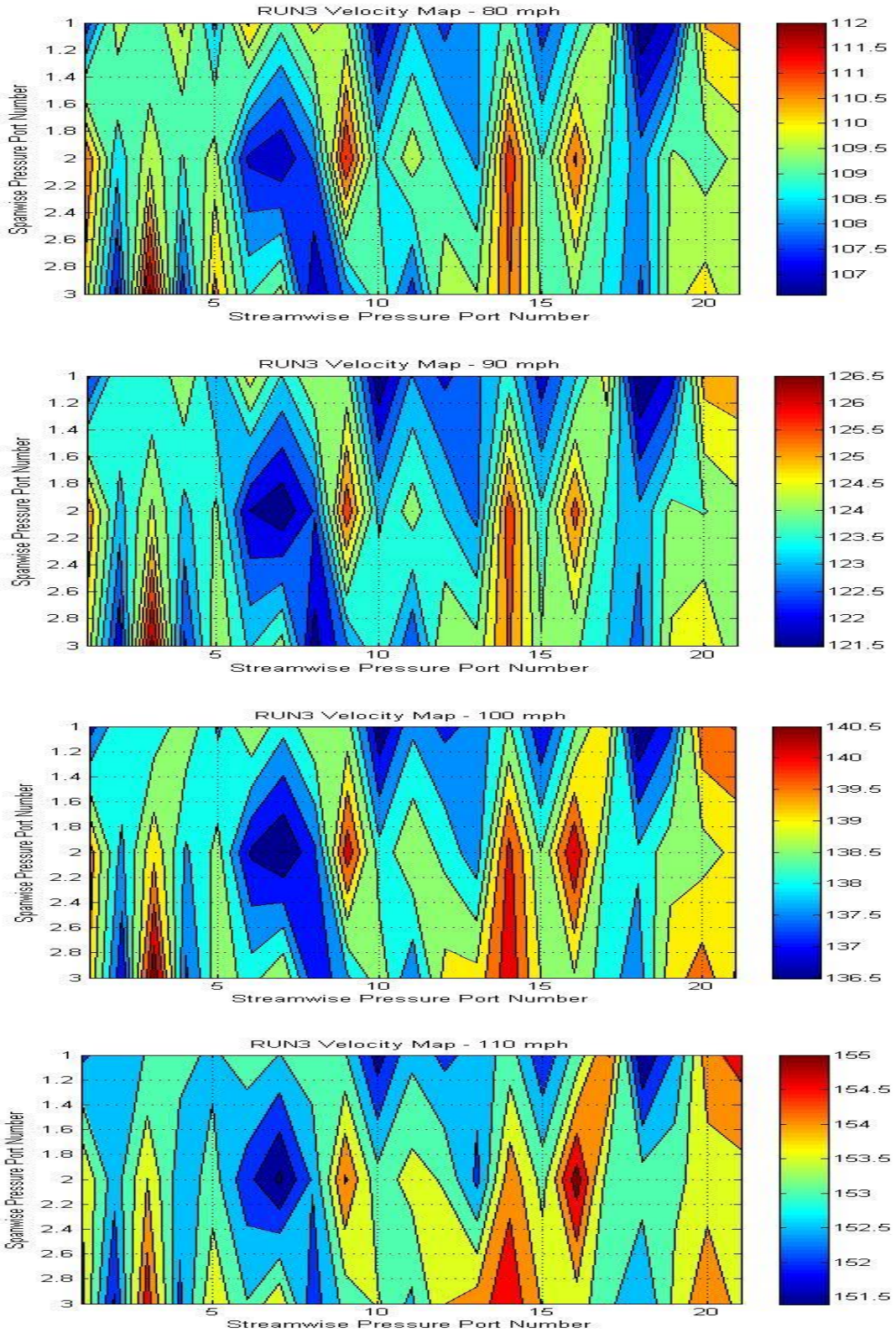

Fig 4.13: Plate 2 Run 3 Velocity Map for 110 mph. Spanwise ports are 1.4 inches apart and streamwise ports are 0.7 inches apart.

Plate 2 shows alternating high and low velocity regions containing closed contours when a VG is present. These high and low velocity regions remain around the same locations over the plate surface even as the tunnel speed increases. Their magnitude with respect to surrounding regions changes slightly. This may be indicative of the progression of stream-wise vortices formed due to the presence of the VG.

The results can be further explained in the following Chapter showing the calculation procedure used within the MATLAB Code as well as the supplementary results for the vortex location and strength calculations. The above $C_{p,}$ and Velocity Maps indicate the possible positions of vortices formed over the flat plate. As the maps are 2 dimensional, they can be considered to be the planar projections of the vortices over them. A rough sketch below (Fig 4.38) shows the flow over a flat plate and the resulting projections of vortices formed over the plate in the form of velocity contours.

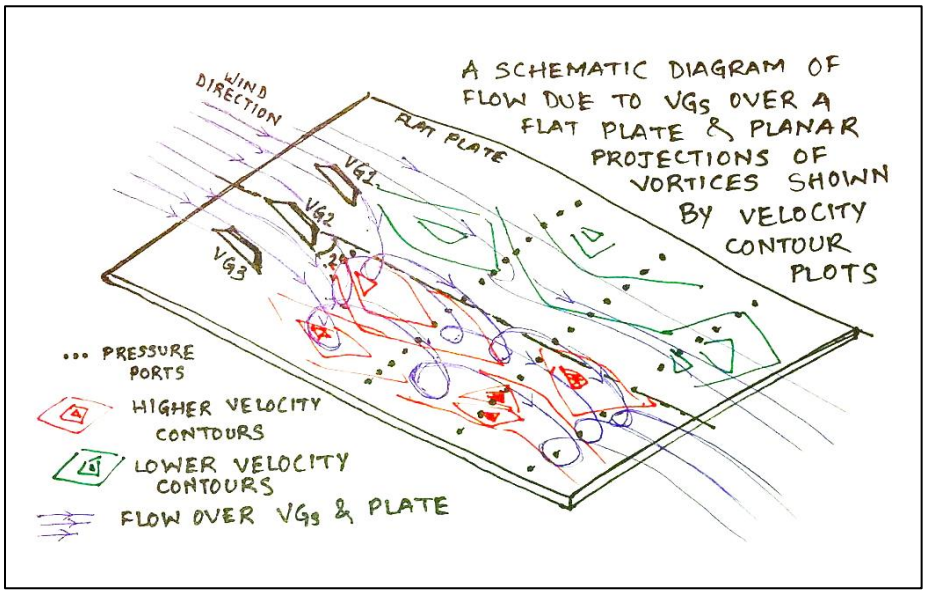

Fig 4.14: A schematic diagram showing the 3D flow over a flat plate and the 2D projection

Borrowing equations from Chapter III:

Circulation: (Γ) = C = V * 2πr

Vorticity: (ω) = V = C/enclosed area

Using the above equations, and the velocity contour plots generated from MATLAB, the projected area below a vortex is taken into consideration and the circulation and normal component of vorticity are calculated in Tables 4.2 and 4.3.

The speeds considered for Plate 1 are 50 mph, 60 mph, 70 mph and 80 mph. The speeds considered for Plate 2 are 80 mph, 90 mph, 100 mph and 110 mph. Considering the increasing velocity plots for Plate 1 - Run 2,

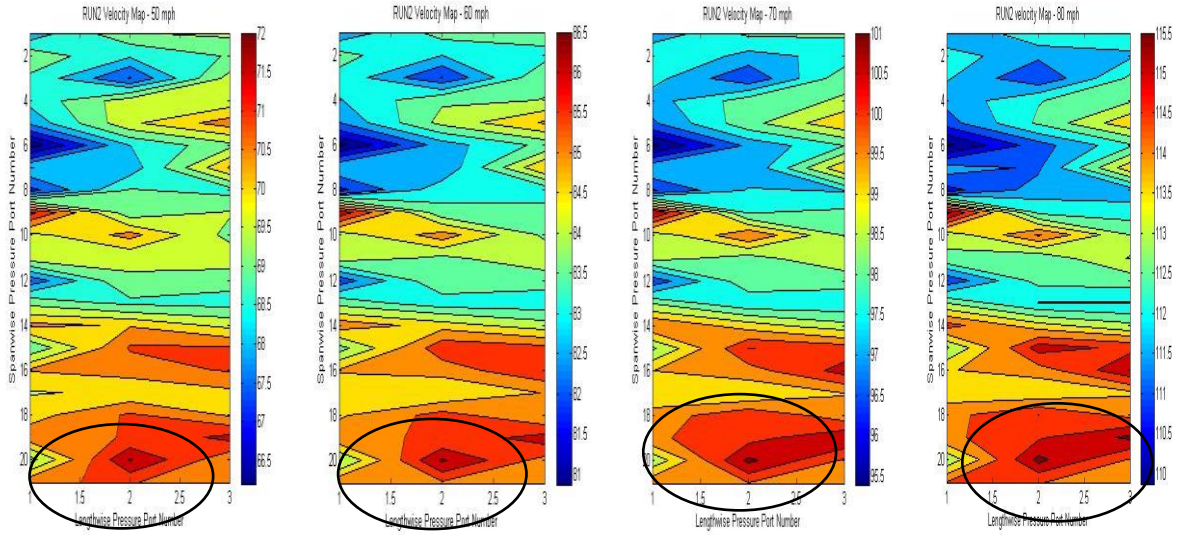

Fig 4.15: Velocity Maps showing increase in observed area for potential vortex location as the speed increases for Plate 1 Run 2

The closed contour higher velocities indicate presence of a vortex over it. The area represented by the 3 red contours (within the marked black circles) can be seen to be increasing with the increase in the speed. The deepest red can be approximated to be the projected center of the vortex as it shows the highest velocity. In order to use the circulation formula, the radius of the vortex can be estimated from the plots.

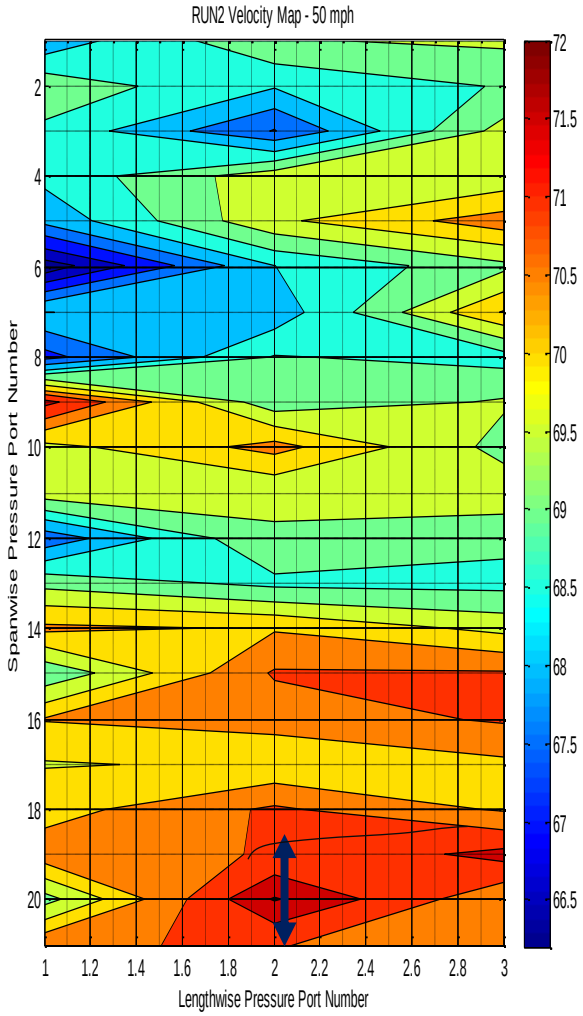

Fig 4.16: Velocity Map for Plate 1 run 2 for speed 50 mph. The arrow indicates the diameter of the contour considered

The marked arrows can be said to give the approximate span of the vortex. The conservative number of ports give jagged contour plots and therefore the arrow can be estimated to give the diameter of the projected vortex.

I have considered a modified contour above (Fig 4.40) as the data points are few and the contour change is abrupt. So, if the arrow gives the diameter of the vortex, the radius and hence the circulation can

be calculated. The tangential velocity considered would be the difference between the velocity at that point and the flow velocity.

Note: for Plate 1, X axis: 1 unit = 2.8 inches and for Y axis: 1 unit = 0.7 inches

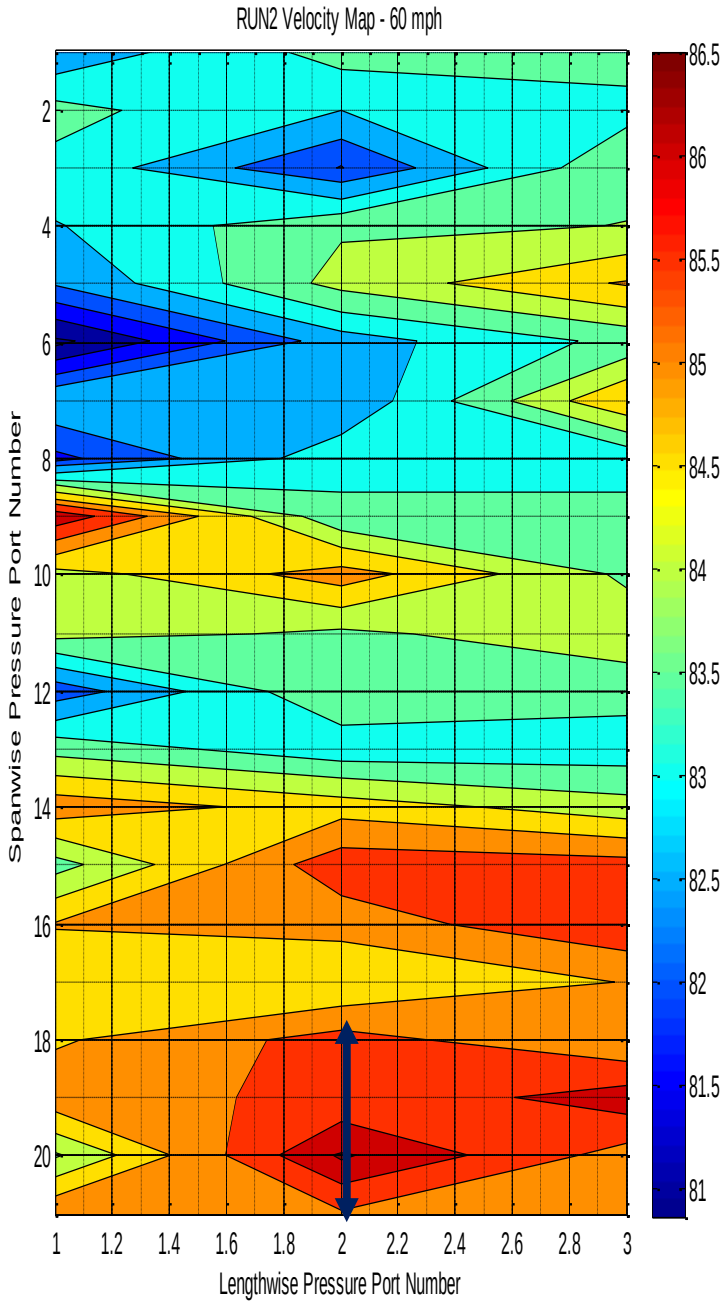

Fig 4.17: Velocity Map for Plate 1 run 2 for speed 60 mph. The arrow indicates the diameter of the contour considered

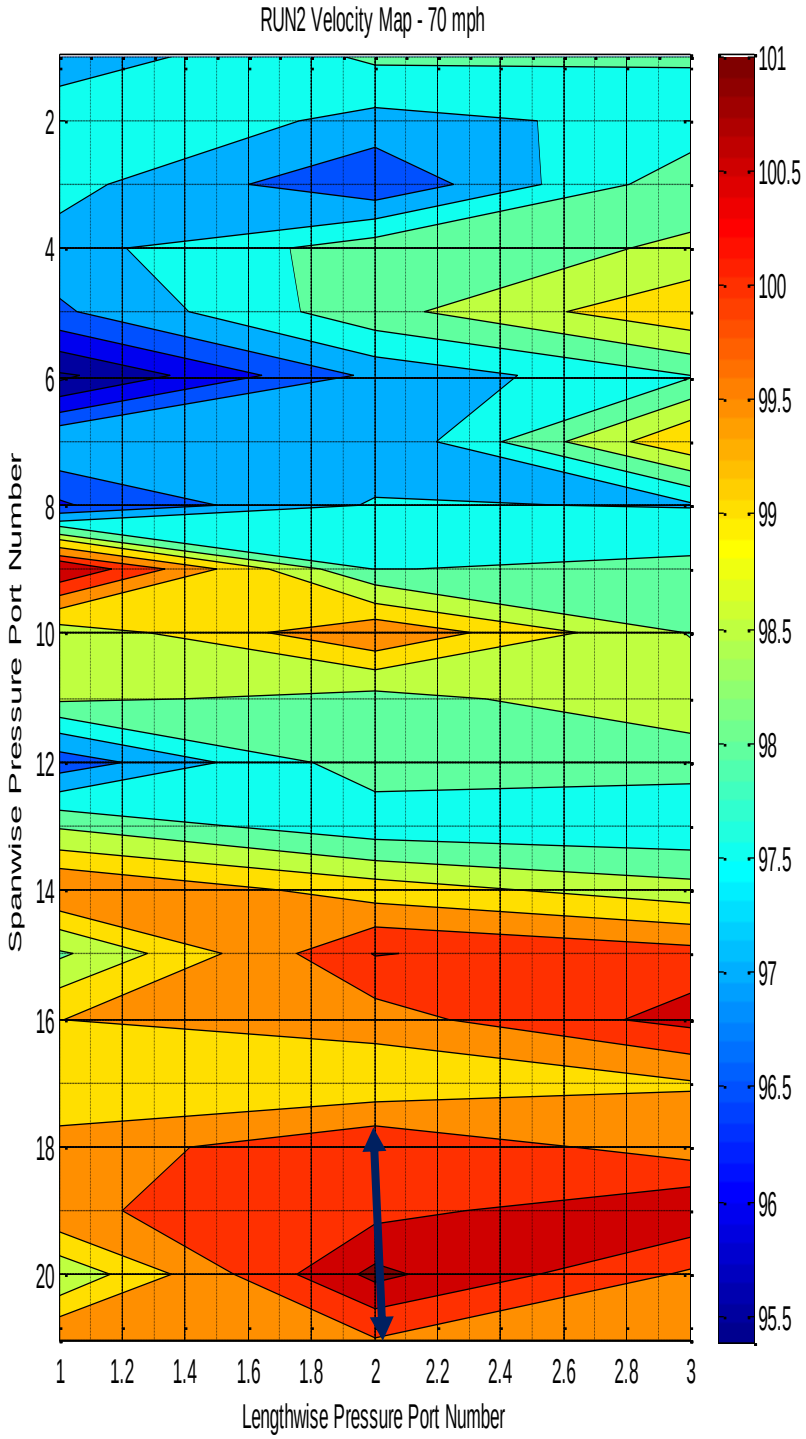

Fig 4.18: Velocity Map for Plate 1 run 2 for speed 70 mph. The arrow indicates the diameter of the contour considered

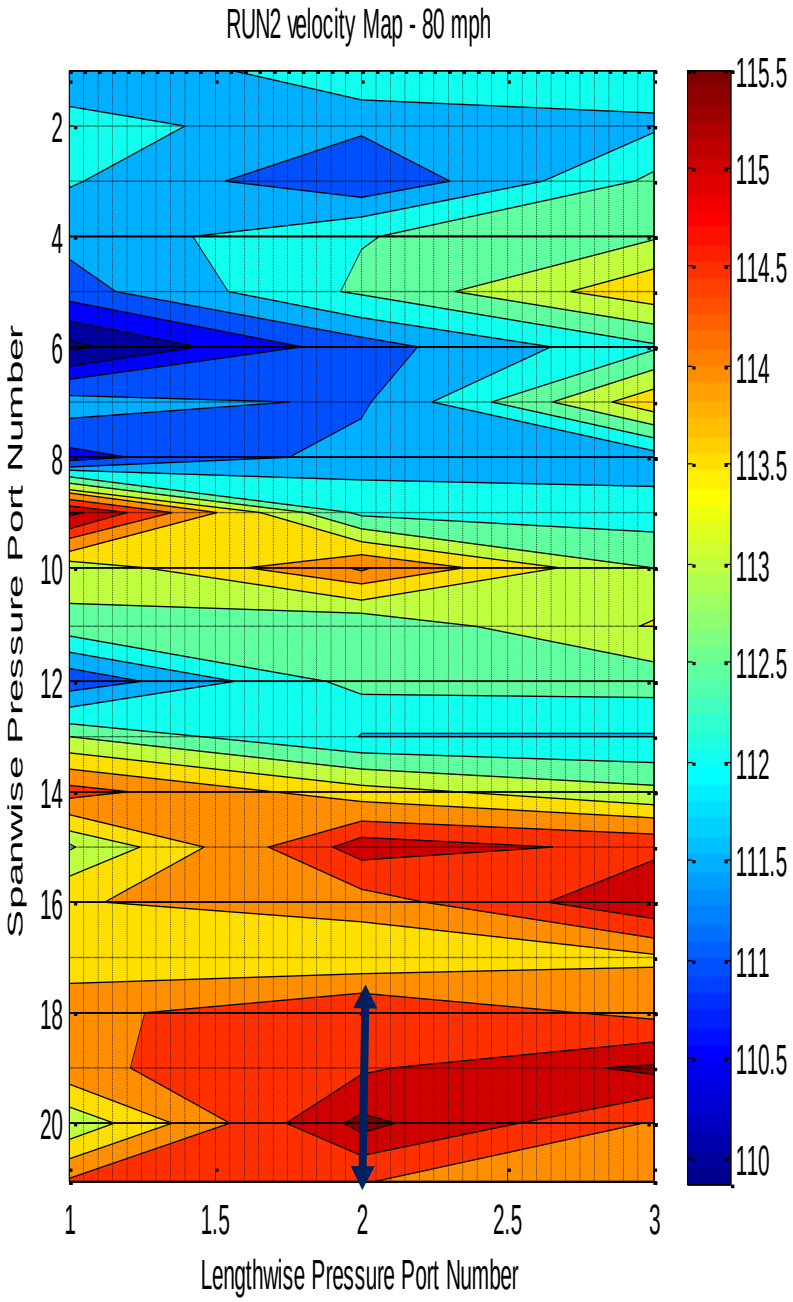

Fig 4.19: Velocity Map for Plate 1 run 2 for speed 80 mph. The arrow indicates the diameter of the contour considered

CIRCULATION & VORTICITY: PLATE 1						
Span (in)	**Radius (in)**	**Flow V (mph)**	**V at point (mph)**	**V Difference (mph)**	**Circulation (in^2/s)**	**Vorticity (/s)**
1.89	0.945	50	71.25	21.25	2170.2	773.5
2.135	1.067	60	85.75	25.75	2970.6	829.7
2.31	1.155	70	100.25	30.25	3775.8	900.9
2.415	1.2075	80	114.75	34.75	4534.7	989.9

Table 4.2: Vorticity and Circulation calculations for Plate 1

For the velocity (V) at point refer to Table 5.1. The vorticity values seem to increase with increase in speed.

Repeating the procedure for Plate 2 (Run 3),

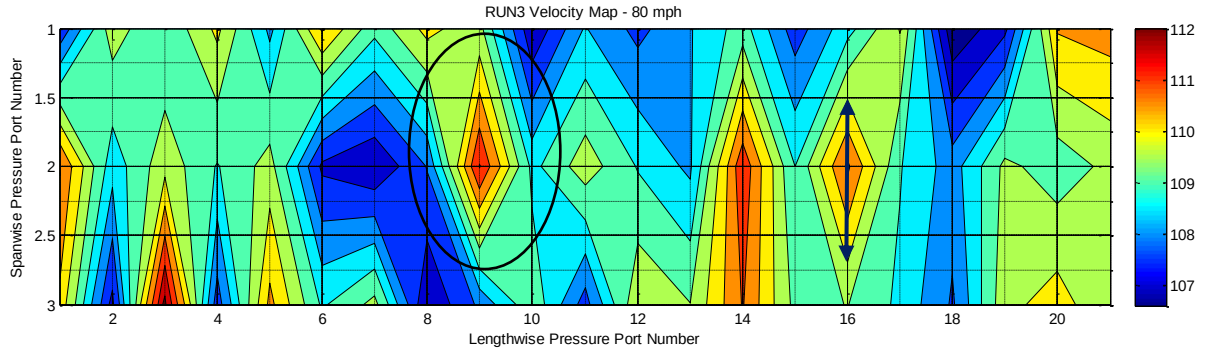

Fig 4.20: Velocity Map for Plate 2 run 3 for speed 80 mph. The arrow indicates the diameter of the contour considered

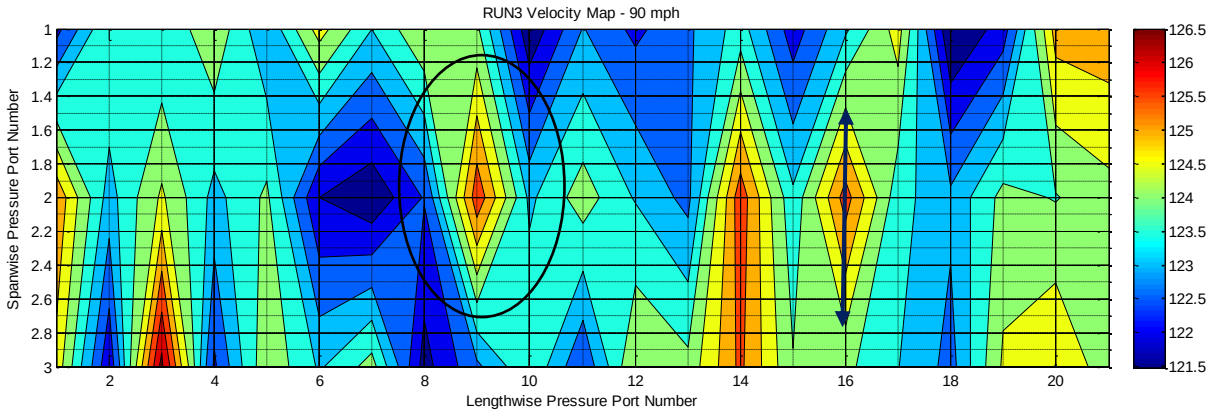

Fig 4.21: Velocity Map for Plate 2 run 3 for speed 90 mph. The arrow indicates the diameter of the contour considered

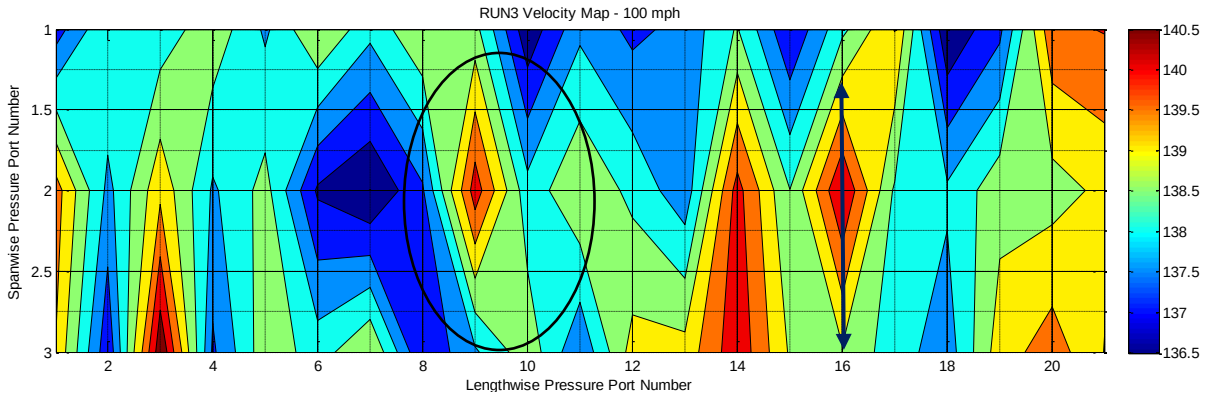

Fig 4.22: Velocity Map for Plate 2 run 3 for speed 100 mph. The arrow indicates the diameter of the contour considered

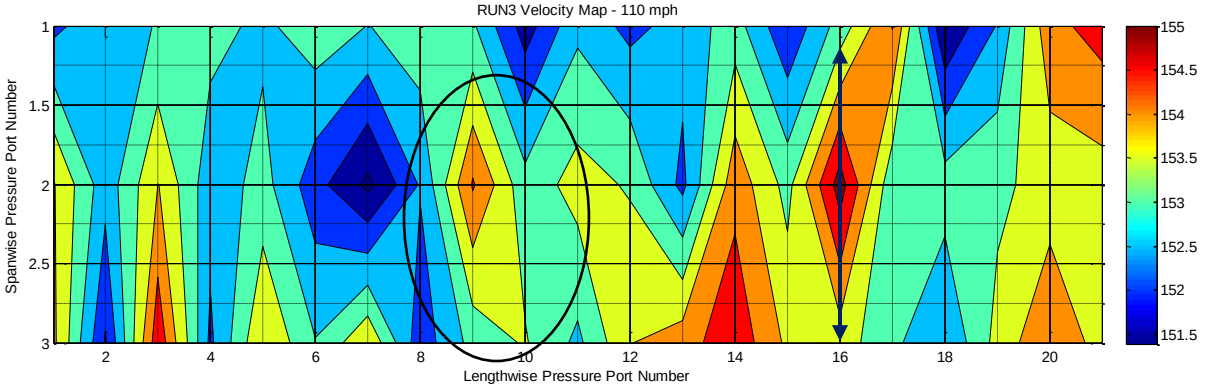

Fig 4.23: Velocity Map for Plate 2 run 3 for speed110 mph. The arrow indicates the diameter of the contour considered

The presence of 2 vortices can be detected here; one marked by the ovals (Vortex 1) and the other by the line measuring its span (Vortex 2). The Vortex 1 is seen to be decreasing in strength as the highest velocity can be seen to be decreasing as the low speed increases. The Vortex 2 seems to be getting stronger with increasing flow speed.

Note: for Plate 1, X axis: 1 unit = 0.7 inches and for Y axis: 1 unit = 1.4 inches

Tabulating the results,

CIRCULATION & VORTICITY: PLATE 2						
Span (in)	**Radius (in)**	**Flow V (mph)**	**V at point (mph)**	**V Difference (mph)**	**Circulation (in^2/s)**	**Vorticity (/s)**
1.75	0.875	80	109.8	29.8	2817	1171
1.875	0.9375	90	124	34	3444	1247
2.1	1.05	100	138.75	38.75	4397	1269
2.5	1.25	110	152.75	42.75	5775	1176

Table 4.3: Vorticity and Circulation calculations for Plate 2

For the velocity (V) at point refer to Table 5.1. The vortex 2 thus seems to increase in strength till 100 mph and then decrease for 110 mph.

The above vorticity magnitude values for the 2 plates were calculated for one sample vortex over the plate. Likewise, every closed contour can be potentially analyzed and the circulation and vorticity can be calculated. The vorticity magnitude values seem comparable to the literature values found in references as follows.

A vorticity of about 3000/s was observed in the case of gas burners with a flow velocity of about 40 mph measured by Particle Image Velocimetry.[18] Vorticity of about 1000 to 1500/s is regularly observed in case of strong winds and typhoons where the velocities are comparable to 100 mph.[19]

Chapter V

Calculation Procedure:

The Kirsten Wind Tunnel Data Acquisition System recorded the following quantities during every test run. For each data point recorded by the tunnel, the Tunnel EPS system processed 500 iterations[20] about the data point and the averaged value was recorded as the output value.

1. Ambient Temperature
2. Ambient Pressure
3. Dynamic Pressure inside test section (Pitot Tube)
4. Coefficients of pressure from the pressure ports
5. Tunnel Fan RPM
6. Wind Speed

The steps followed in the calculations are as follows:

1. Plot the *Cp* map for the data from the wind tunnel values
2. Calculate the air density from ambient pressure and temperature
3. Use *Cp* values and tunnel speed to calculate velocities at ports
4. Plot the Velocity Map for the cases
5. Calculate the closed loop area over the pressure & velocity
6. Using this area, calculate the circulation and normal component of vorticity

Velocity at pressure ports:

If the velocity and pressure variations are negligible as compared to the speed of sound, the following relationship[21] is valid for the flow of incompressible fluids where variations in speed and pressure are sufficiently small that variations in fluid density can be neglected. This is a reasonable assumption when the Mach number is less than about 0.3.

$$C_p = 1 - (\frac{u}{u_\infty})^2$$

Where

u = flow speed at the point where pressure coefficient is measured

u_∞ = free stream velocity = V_∞

The following table gives the values for the velocities and pressures at each of the ports for various speeds. The QA (psf) and the corresponding V_infinity (mph) values are the tunnel run values from 10 – 110 mph and are used for the calculation procedure.

QA (psf)	**QA (Pa)**	**V_infinity (mph)**	**V_infinity (mps)**
0.248	11.87	10	4.47
0.998	47.78	20	8.94
2.239	107.2	30	13.41
3.973	190.23	40	17.88
6.241	298.8	50	22.35
8.899	426	60	26.82
12.24	586.1	70	31.29
15.86	759.7	80	35.76
19.86	950.9	90	40.23
24.48	1172.2	100	44.70
29.73	1423.7	110	49.17

Table 5.1: Velocities at ports for tunnel speeds

MATLAB Code Explanation:

Pressure Coefficient Map: This part of the code rearranges the pressure coefficient values obtained from the tunnel into individual matrices according to the speed and contour plots of these matrices are generated. The plots show the entire surface of the plate and the axes indicate the pressure port locations.

```
%  CP Map %
RUN1_1 = [RUN1(1,1:21);RUN1(1,22:42);RUN1(1,43:63)]';
RUN1_2 = [RUN1(2,1:21);RUN1(2,22:42);RUN1(2,43:63)]';
RUN1_3 = [RUN1(3,1:21);RUN1(3,22:42);RUN1(3,43:63)]';

figure; contourf(RUN1_1);colorbar; title('RUN1 Cp Map - 10 mph');set(gca,'YDir','Reverse')
figure; contourf(RUN1_2);colorbar; title('RUN1 Cp Map - 20 mph');set(gca,'YDir','Reverse')
figure; contourf(RUN1_3);colorbar; title('RUN1 Cp Map - 30 mph');set(gca,'YDir','Reverse')
```

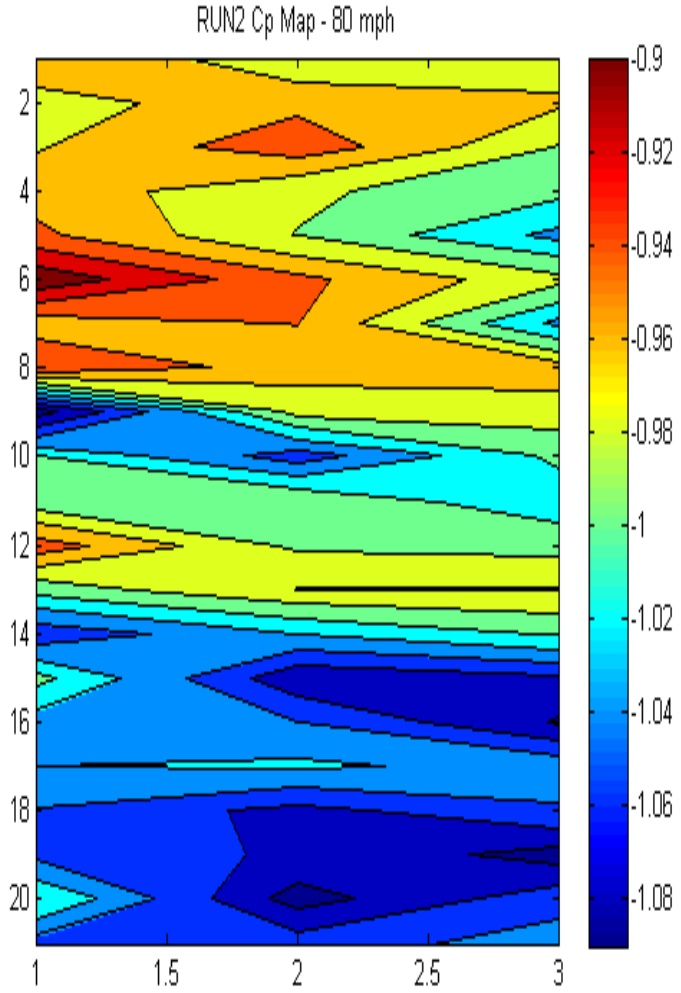

Fig 5.1: *Cp* Map for Plate 1 with pressure port locations indicated.

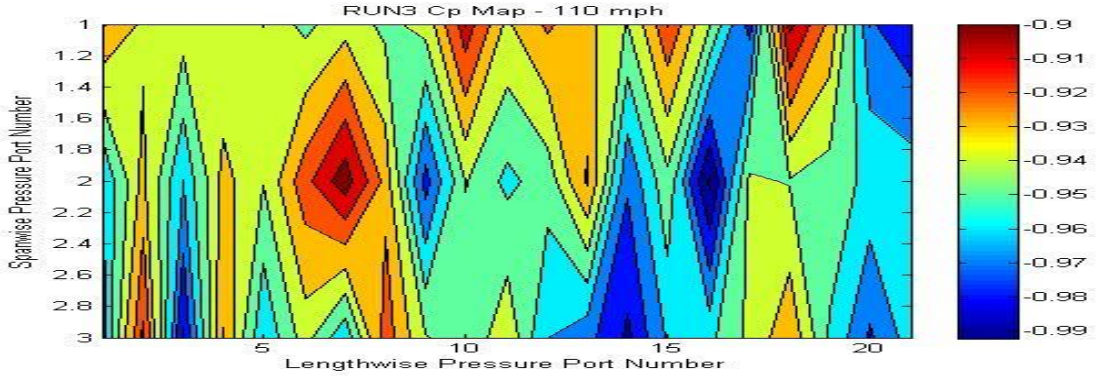

Fig 5.2: *Cp* Map for Plate 2 with pressure port locations indicated.

For Plate 1, the vertical distance between two ports is 0.7 inches and the horizontal distance between two ports is 2.8 inches.

For Plate 2, the vertical distance between two ports is 1.4 inches and the horizontal distance between two ports is 0.7 inches.

Velocity Map: This part of the code uses the pressure coefficient values to calculate the velocity values as described above, arranges into individual matrices according to the speed and contour plots of these matrices are generated. The plots show the entire surface of the plate and the axes indicate the pressure port locations.

```
%Velocity Map - RUN1 %

V1_1 = 10 * sqrt(1-RUN1_1);
V1_2 = 20 * sqrt(1-RUN1_2);
V1_3 = 30 * sqrt(1-RUN1_3);
V1_4 = 40 * sqrt(1-RUN1_4);

figure; contourf(V1_1);colorbar; title('RUN1 velocity Map - 10 mph');
   set(gca,'YDir','Reverse');xlabel('Lengthwise Pressure Port Number');
   ylabel('Spanwise Pressure Port Number');
figure; contourf(V1_2);colorbar; title('RUN1 Velocity Map - 20 mph');
   set(gca,'YDir','Reverse');xlabel('Lengthwise Pressure Port Number');
   ylabel('Spanwise Pressure Port Number');
figure; contourf(V1_3);colorbar; title('RUN1 Velocity Map - 30 mph');
   set(gca,'YDir','Reverse');xlabel('Lengthwise Pressure Port Number');
   ylabel('Spanwise Pressure Port Number');
```

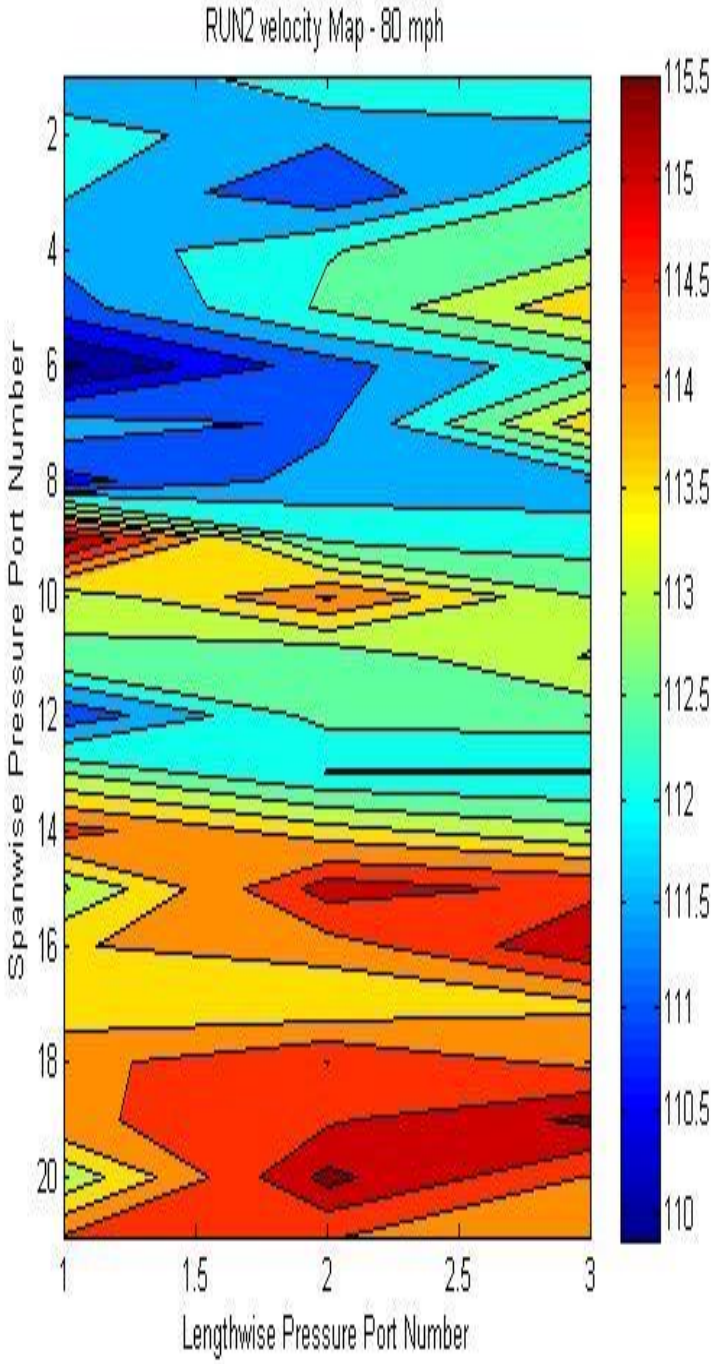

Fig 5.3: Velocity Map for Plate 1 with pressure port locations indicated.

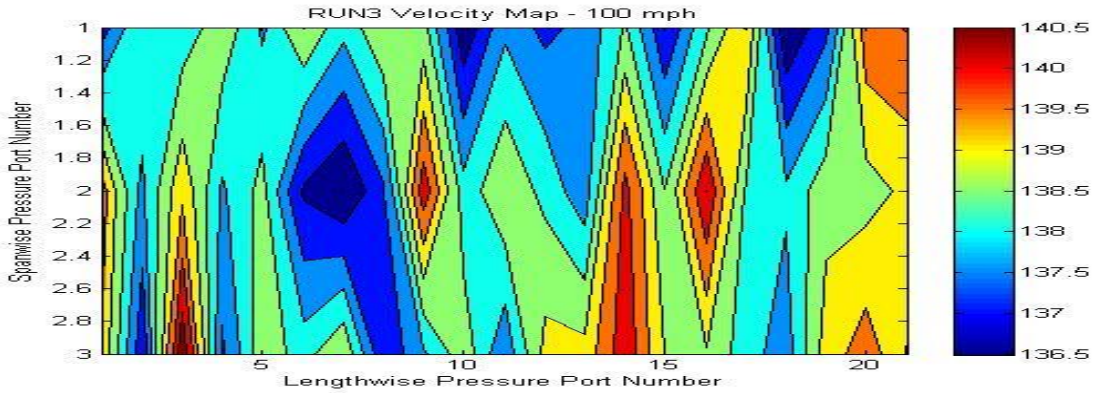

Fig 5.4: Velocity Map for Plate2 with pressure port locations indicated.

For Plate 1, the vertical distance between two ports is 0.7 inches and the horizontal distance between two ports is 2.8 inches.

For Plate 2, the vertical distance between two ports is 1.4 inches and the horizontal distance between two ports is 0.7 inches.

Chapter VI

Discussion & Analysis

This study has been a progression though the iterations 1, 2 and 3 where, in iteration 1, five types of VGs were tested for different flow speeds. These tests were carried out in the University of Washington's Low-Speed Wind Tunnel (LWT) and it was found that the pressure sensing equipment was not sensitive enough to arrive at conclusive results. The iteration 2 was a repetition of iteration 1, but the test were carried out in the Kirsten Wind Tunnel (KWT). Here, the five different types of VGs were tested at similar flow conditions to do a comparative study on the flow behavior due to the VGs. The results from this iteration proved that the geometry and positioning of the VGs are critical parameters that affect the nature of the flow. The iteration 3 was based on iteration 2 as it used the most optimum functioning VG from the five used in iteration 2. The flow conditions, geometry of the plates and the geometry and positioning of the VGs were parameters that were studied and decided through the past experiment iterations and the literature review.

Through iteration 3, it was seen that pressure coefficient and velocity contour plots can be used to detect the flow variations over the plate surface. The Plate 1 plots were used to study the span-wise vortices formed due to 3 VGs. The Plate 2 plots were used to study the stream-wise vortices formed due to a single VG over a long, narrow plate. The flow patterns could be seen getting affected by the increase in flow speeds and the vortices were observed to either grow or shrink in size or strengthen and weaken. The circulation and normal component of vorticity could be calculated through simple geometric calculations. The plots may be slightly crude owing to the limited number of sensing ports, but they gave an opportunity to detect, calculate and compare the circulation and vorticity across various speeds and plates. This method of calculation has a lot of scope for refinement.

Chapter VII

Conclusions

The VG and no VG data was used to plot the pressure coefficient and velocity contour plots. The contour plots were used to compare the “with” and “without” VG cases for both the plates. Even though the no VG case showed pressure coefficient and velocity fluctuations, they were considered to be existent in both the VG and non VG due to similar flow and tunnel conditions. Despite the flow conditions being kept exactly same, there is clear and stronger variation seen in the Runs with VGs.

The results and plots obtained from this thesis can be used to visualize the development of flow over a flat plate for various speeds. The pressure coefficient and velocity maps can help indicate the possible vortex locations over the plate as also calculate the normal component of vorticity. Vorticity values were found comparable to similar other case studies. It can be thus concluded that the pressure measurements can facilitate vortex detection.

The study also delves into the factors that influence the flow generated by VGs, these being the geometry of the VG and its positioning on the plate. The experimental analysis can help in deciding the appropriate vortex generator geometry required for the flow analysis. There is not much literature available on trapezoidal vane type vortex generators and this study attempted their use. The study also was a lesson in importance of correct measuring/ sensing equipment and its criticality influencing the quality of results as shown in iterations 1 & 2 where the results obtained were not satisfactory/conclusive due to improper sensing equipment used.

Chapter VIII

Future Scope

Vortex detection in terms of its location and magnitude is an important step in the study of vortices and the way they influence the air flow around them. This information can be used to either generate or control or do away with the vortices according to the required need and a better understanding of flow over any object can be developed. This can help in controlling the boundary layer separation and the subsequent drag generated as a result of it leading to an increased efficiency of applications.

The experimental setup used in this study can be extended in the following ways:

- Airfoil shaped body can be used instead of a flat plate
- Different geometries of vortex generators can be tested
- The yaw angle of vortex generators can be changed. There is also a scope of using an active control vortex generator set
- The flow visualization can be bettered. 3 dimensional flow visualization techniques can be used which can help determine the total magnitude of vorticity
- An active feedback control system can be used to change the plate yaw angle in order to potentially hold the developed vortices in places (stationary vortices). This will ensure that the boundary layer separation can be totally avoided

References:

1. Aircraft Controls - Leroy R. Grumman Cadet Squadron – http://www.cap-ny153.org/aircraftcontrols.htm
2. Smith F T 1994 *Journal of Fluid Mechanics* 270 91–131
3. Velte C M, Hansen M O L and Okulov V L 2009 *Journal of Fluid Mechanics* 619 167–177
4. Taylor H D 1947 The elimination of diffuser separation by vortex generators Research department report no. r-4012-3 United Aircraft Corporation, East Hartford, Connecticut

   Taylor H D 1948 Application of vortex generator mixing principles to diffusers Research department concluding report no. r-15064-5 United Aircraft Corporation, East Hartford, Connecticut

   Taylor H D 1950 Summary report on vortex generators Research department report no. r-05280-9 United Aircraft Corporation, East Hartford, Connecticut
5. Schubauer G B and Spangenber W G 1960 *Journal of Fluid Mechanics* 8 10–32
6. Fern´andez-G´amiz U, Velte C M, R´ethor´e P E and Sørensen N N 2012 Self-similarity and helical symmetry in vortex generator flow simulations
7. Hyoung S. Chung , Christopher A. Seaver and Thomas E. McLaughlin - Vortex Flow Control Over a Delta Wing By Co-Rotating and Counter-Rotating Vortex Generator *28th AIAA Applied Aerodynamics Conference*
8. Masaru KOIKE, Tsunehisa NAGAYOSHI and Naoki HAMAMOTO - Research on Aerodynamic Drag Reduction by Vortex Generators *Mitsubishi Motors Technical Review 2004 No. 16*
9. H. Tebbiche, M.S. Boutoudj - Optimized vortex generators in the flow separation control around a NACA 0015 profile *Proceedings of the 9th International Conference on Structural Dynamics, EURODYN 2014 Porto, Portugal*, 30 June - 2 July 2014

10. HO-JOON SHIM, KI-JUNG KWON, and SEUNG-O PARK - Experimental Study on the Wake Characteristics of Vane-Type Vortex Generators in a Flat Plate Turbulent Boundary Layer *Recent Advances in Fluid Mechanics and Thermal Engineering*

11. U. Fern´andez-G´amiz, G. Zamorano and E. Zulueta - Computational study of the vortex path variation with the VG height *Journal of Physics: Conference Series, Volume 524, conference 1*
12. Pressure Coefficient - http://www.liquisearch.com/pressure_coefficient
13. Circulation & Vorticity – Lecture 4 – http://www.ess.uci.edu/~yu/class/ess228/lecture.4.vorticity.all.pdf
14. Circulation - https://en.wikipedia.org/wiki/Circulation_(fluid_dynamics) Vorticity – https://en.wikipedia.org/wiki/Vorticity
15. Kirsten Wind Tunnel – University of Washington, Seattle – https://www.aa.washington.edu/AERL/KWT
16. Electronic pressure scanning system - Kirsten Wind Tunnel – University of Washington, Seattle – https://www.aa.washington.edu/AERL/KWT
17. Scanivalve ZOC 23 - http://scanivalve.com/products/pressure-measurement/miniature-analog-pressure-scanners/zoc23b-miniature-pressure-scanner/
18. Particle Image Velocimetry: New Developments and Recent Applications - edited by Andreas Schröder, Christian E. Willert
19. Alexandre Olivier Fierro – High resolution Simulation of the Microphysics and Electrification in Hurricane-like vortices over warm ocean & landfall, 2007
20. Kirsten Wind Tunnel – University of Washington, Seattle – https://www.aa.washington.edu/AERL/KWT
21. Pressure coefficient - https://en.wikipedia.org/wiki/Pressure_coefficient
22. Low-speed Wind Tunnel – University of Washington – https://www.aa.washington.edu/AERL/LSWT

Appendix i

MATLAB Code for Data Processing

The MATLAB Code used in thesis is presented ahead. The code is used to process the data obtained from the wind tunnel data acquisition system and is used to do the following:

1. Rearrange the obtained data to represent individual Runs and speeds for each run
2. Plot the pressure coefficient maps from the data for each speed and run
3. Plot the pressure differential maps from the data for each speed and run
4. Plot the velocity magnitude maps from the data for each speed and run

```
% Run1 : Plate 1 - no VGs
% Run2 : Plate 1 - with VGs
% Run3 : Plate 2 - with VG
% Run4 : Plate 2 - no VG


% Columnwise Cp Plot %
figure;
hold all;
for k=5:8
    plot(RUN1(k,1:21));
    legend('50 mph','60 mph',...
        '70 mph','80 mph', 'Location','southeast');
    title('Run 1 - Cp variation with Speed - Column 1');
    xlabel('Spanwise Pressure Port Number');
    ylabel('Cp Value');
end
figure;
hold all;
for k=5:8
    plot(RUN2(k,1:21));
    legend('50 mph','60 mph',...
        '70 mph','80 mph', 'Location','southeast');
    title('Run 2 - Cp variation with Speed - Column 1');
    xlabel('Spanwise Pressure Port Number');
    ylabel('Cp Value');
end

figure;
hold all;
for k=5:8
    plot(RUN1(k,22:42));
    legend('50 mph','60 mph',...
        '70 mph','80 mph', 'Location','southeast');
    title('Run 1 - Cp variation with Speed - Column 2');
    xlabel('Spanwise Pressure Port Number');
    ylabel('Cp Value');
end
figure;
hold all;
for k=5:8
    plot(RUN2(k,22:42));
    legend('50 mph','60 mph',...
        '70 mph','80 mph', 'Location','southeast');
    title('Run 2 - Cp variation with Speed - Column 2');
    xlabel('Spanwise Pressure Port Number');
    ylabel('Cp Value');
end

figure;
hold all;
for k=5:8
    plot(RUN1(k, 43:63));
```

```
    legend('50 mph','60 mph',...
        '70 mph','80 mph', 'Location','southeast');
    title('Run 1 - Cp variation with Speed - Column 3');
    xlabel('Spanwise Pressure Port Number');
    ylabel('Cp Value');
end
figure;
hold all;
for k=5:8
    plot(RUN2(k,43:63));
    legend('50 mph','60 mph',...
        '70 mph','80 mph', 'Location','southeast');
    title('Run 2 - Cp variation with Speed - Column 3');
    xlabel('Spanwise Pressure Port Number');
    ylabel('Cp Value');
end

%  CP Map %
RUN1_1 = [RUN1(1,1:21);RUN1(1,22:42);RUN1(1,43:63)]';
RUN1_2 = [RUN1(2,1:21);RUN1(2,22:42);RUN1(2,43:63)]';
RUN1_3 = [RUN1(3,1:21);RUN1(3,22:42);RUN1(3,43:63)]';
RUN1_4 = [RUN1(4,1:21);RUN1(4,22:42);RUN1(4,43:63)]';
RUN1_5 = [RUN1(5,1:21);RUN1(5,22:42);RUN1(5,43:63)]';
RUN1_6 = [RUN1(6,1:21);RUN1(6,22:42);RUN1(6,43:63)]';
RUN1_7 = [RUN1(7,1:21);RUN1(7,22:42);RUN1(7,43:63)]';
RUN1_8 = [RUN1(8,1:21);RUN1(8,22:42);RUN1(8,43:63)]';

figure; contourf(RUN1_1);colorbar; title('RUN1 Cp Map - 10 mph');
    set(gca,'YDir','Reverse');
    xlabel('Streamwise Pressure Port Number');
    ylabel('Spanwise Pressure Port Number');
figure; contourf(RUN1_2);colorbar; title('RUN1 Cp Map - 20 mph');
    set(gca,'YDir','Reverse');
    xlabel('Streamwise Pressure Port Number');
    ylabel('Spanwise Pressure Port Number');
figure; contourf(RUN1_3);colorbar; title('RUN1 Cp Map - 30 mph');
    set(gca,'YDir','Reverse');
    xlabel('Streamwise Pressure Port Number');
    ylabel('Spanwise Pressure Port Number');
figure; contourf(RUN1_4);colorbar; title('RUN1 Cp Map - 40 mph');
    set(gca,'YDir','Reverse');
    xlabel('Streamwise Pressure Port Number');
    ylabel('Spanwise Pressure Port Number');
figure; contourf(RUN1_5);colorbar; title('RUN1 Cp Map - 50 mph');
    set(gca,'YDir','Reverse');
    xlabel('Streamwise Pressure Port Number');
    ylabel('Spanwise Pressure Port Number');
figure; contourf(RUN1_6);colorbar; title('RUN1 Cp Map - 60 mph');
    set(gca,'YDir','Reverse');
    xlabel('Streamwise Pressure Port Number');
    ylabel('Spanwise Pressure Port Number');
figure; contourf(RUN1_7);colorbar; title('RUN1 Cp Map - 70 mph');
    set(gca,'YDir','Reverse');
    xlabel('Streamwise Pressure Port Number');
```

```
    ylabel('Spanwise Pressure Port Number');
figure; contourf(RUN1_8);colorbar; title('RUN1 Cp Map - 80 mph');
    set(gca,'YDir','Reverse');
    xlabel('Streamwise Pressure Port Number');
    ylabel('Spanwise Pressure Port Number');
```

```
RUN2_1 = [RUN2(1,1:21);RUN2(1,22:42);RUN2(1,43:63)]';
RUN2_2 = [RUN2(2,1:21);RUN2(2,22:42);RUN2(2,43:63)]';
RUN2_3 = [RUN2(3,1:21);RUN2(3,22:42);RUN2(3,43:63)]';
RUN2_4 = [RUN2(4,1:21);RUN2(4,22:42);RUN2(4,43:63)]';
RUN2_5 = [RUN2(5,1:21);RUN2(5,22:42);RUN2(5,43:63)]';
RUN2_6 = [RUN2(6,1:21);RUN2(6,22:42);RUN2(6,43:63)]';
RUN2_7 = [RUN2(7,1:21);RUN2(7,22:42);RUN2(7,43:63)]';
RUN2_8 = [RUN2(8,1:21);RUN2(8,22:42);RUN2(8,43:63)]';

figure; contourf(RUN2_1);colorbar; title('RUN2 Cp Map - 10 mph');
    set(gca,'YDir','Reverse');
    xlabel('Streamwise Pressure Port Number');
    ylabel('Spanwise Pressure Port Number');
figure; contourf(RUN2_2);colorbar; title('RUN2 Cp Map - 20 mph');
    set(gca,'YDir','Reverse');
    xlabel('Streamwise Pressure Port Number');
    ylabel('Spanwise Pressure Port Number');
figure; contourf(RUN2_3);colorbar; title('RUN2 Cp Map - 30 mph');
    set(gca,'YDir','Reverse');
    xlabel('Streamwise Pressure Port Number');
    ylabel('Spanwise Pressure Port Number');
figure; contourf(RUN2_4);colorbar; title('RUN2 Cp Map - 40 mph');
    set(gca,'YDir','Reverse');
    xlabel('Streamwise Pressure Port Number');
    ylabel('Spanwise Pressure Port Number');
figure; contourf(RUN2_5);colorbar; title('RUN2 Cp Map - 50 mph');
    set(gca,'YDir','Reverse');
    xlabel('Streamwise Pressure Port Number');
    ylabel('Spanwise Pressure Port Number');
figure; contourf(RUN2_6);colorbar; title('RUN2 Cp Map - 60 mph');
    set(gca,'YDir','Reverse');
    xlabel('Streamwise Pressure Port Number');
    ylabel('Spanwise Pressure Port Number');
figure; contourf(RUN2_7);colorbar; title('RUN2 Cp Map - 70 mph');
    set(gca,'YDir','Reverse');
    xlabel('Streamwise Pressure Port Number');
    ylabel('Spanwise Pressure Port Number');
figure; contourf(RUN2_8);colorbar; title('RUN2 Cp Map - 80 mph');
    set(gca,'YDir','Reverse');
    xlabel('Streamwise Pressure Port Number');
    ylabel('Spanwise Pressure Port Number');
```

```
RUN3_1 = reshape(RUN3(1,:),3,[]);
RUN3_2 = reshape(RUN3(2,:),3,[]);
RUN3_3 = reshape(RUN3(3,:),3,[]);
RUN3_4 = reshape(RUN3(4,:),3,[]);
RUN3_5 = reshape(RUN3(5,:),3,[]);
RUN3_6 = reshape(RUN3(6,:),3,[]);
```

```
RUN3_7 = reshape(RUN3(7,:),3,[]);
RUN3_8 = reshape(RUN3(8,:),3,[]);
RUN3_9 = reshape(RUN3(9,:),3,[]);
RUN3_10 = reshape(RUN3(10,:),3,[]);
RUN3_11 = reshape(RUN3(11,:),3,[]);

figure; contourf(RUN3_1);colorbar; title('RUN3 Cp Map - 10 mph');
    set(gca,'YDir','Reverse');
    xlabel('Streamwise Pressure Port Number');
    ylabel('Spanwise Pressure Port Number');
figure; contourf(RUN3_2);colorbar; title('RUN3 Cp Map - 20 mph');
    set(gca,'YDir','Reverse');
    xlabel('Streamwise Pressure Port Number');
    ylabel('Spanwise Pressure Port Number');
figure; contourf(RUN3_3);colorbar; title('RUN3 Cp Map - 30 mph');
    set(gca,'YDir','Reverse');
    xlabel('Streamwise Pressure Port Number');
    ylabel('Spanwise Pressure Port Number');
figure; contourf(RUN3_4);colorbar; title('RUN3 Cp Map - 40 mph');
    set(gca,'YDir','Reverse');
    xlabel('Streamwise Pressure Port Number');
    ylabel('Spanwise Pressure Port Number');
figure; contourf(RUN3_5);colorbar; title('RUN3 Cp Map - 50 mph');
    set(gca,'YDir','Reverse');
    xlabel('Streamwise Pressure Port Number');
    ylabel('Spanwise Pressure Port Number');
figure; contourf(RUN3_6);colorbar; title('RUN3 Cp Map - 60 mph');
    set(gca,'YDir','Reverse');
    xlabel('Streamwise Pressure Port Number');
    ylabel('Spanwise Pressure Port Number');
figure; contourf(RUN3_7);colorbar; title('RUN3 Cp Map - 70 mph');
    set(gca,'YDir','Reverse');
    xlabel('Streamwise Pressure Port Number');
    ylabel('Spanwise Pressure Port Number');
figure; contourf(RUN3_8);colorbar; title('RUN3 Cp Map - 80 mph');
    set(gca,'YDir','Reverse');
    xlabel('Streamwise Pressure Port Number');
    ylabel('Spanwise Pressure Port Number');
figure; contourf(RUN3_9);colorbar; title('RUN3 Cp Map - 90 mph');
    set(gca,'YDir','Reverse');
    xlabel('Streamwise Pressure Port Number');
    ylabel('Spanwise Pressure Port Number');
figure; contourf(RUN3_10);colorbar; title('RUN3 Cp Map - 100 mph');
    set(gca,'YDir','Reverse');
    xlabel('Streamwise Pressure Port Number');
    ylabel('Spanwise Pressure Port Number');
figure; contourf(RUN3_11);colorbar; title('RUN3 Cp Map - 110 mph');
    set(gca,'YDir','Reverse');
    xlabel('Streamwise Pressure Port Number');
    ylabel('Spanwise Pressure Port Number');
```

```
RUN4_1 = reshape(RUN4(1,:),3,[]);
RUN4_2 = reshape(RUN4(2,:),3,[]);
RUN4_3 = reshape(RUN4(3,:),3,[]);
```

```
RUN4_4 = reshape(RUN4(4,:),3,[]);
RUN4_5 = reshape(RUN4(5,:),3,[]);
RUN4_6 = reshape(RUN4(6,:),3,[]);
RUN4_7 = reshape(RUN4(7,:),3,[]);
RUN4_8 = reshape(RUN4(8,:),3,[]);
RUN4_9 = reshape(RUN4(9,:),3,[]);
RUN4_10 = reshape(RUN4(10,:),3,[]);
RUN4_11 = reshape(RUN4(11,:),3,[]);

figure; contourf(RUN4_1);colorbar; title('RUN4 Cp Map - 10 mph');
    set(gca,'YDir','Reverse');
    xlabel('Streamwise Pressure Port Number');
    ylabel('Spanwise Pressure Port Number');
figure; contourf(RUN4_2);colorbar; title('RUN4 Cp Map - 20 mph');
    set(gca,'YDir','Reverse');
    xlabel('Streamwise Pressure Port Number');
    ylabel('Spanwise Pressure Port Number');
figure; contourf(RUN4_3);colorbar; title('RUN4 Cp Map - 30 mph');
    set(gca,'YDir','Reverse');
    xlabel('Streamwise Pressure Port Number');
    ylabel('Spanwise Pressure Port Number');
figure; contourf(RUN4_4);colorbar; title('RUN4 Cp Map - 40 mph');
    set(gca,'YDir','Reverse');
    xlabel('Streamwise Pressure Port Number');
    ylabel('Spanwise Pressure Port Number');
figure; contourf(RUN4_5);colorbar; title('RUN4 Cp Map - 50 mph');
    set(gca,'YDir','Reverse');
    xlabel('Streamwise Pressure Port Number');
    ylabel('Spanwise Pressure Port Number');
figure; contourf(RUN4_6);colorbar; title('RUN4 Cp Map - 60 mph');
    set(gca,'YDir','Reverse');
    xlabel('Streamwise Pressure Port Number');
    ylabel('Spanwise Pressure Port Number');
figure; contourf(RUN4_7);colorbar; title('RUN4 Cp Map - 70 mph');
    set(gca,'YDir','Reverse');
    xlabel('Streamwise Pressure Port Number');
    ylabel('Spanwise Pressure Port Number');
figure; contourf(RUN4_8);colorbar; title('RUN4 Cp Map - 80 mph');
    set(gca,'YDir','Reverse');
    xlabel('Streamwise Pressure Port Number');
    ylabel('Spanwise Pressure Port Number');
figure; contourf(RUN4_9);colorbar; title('RUN4 Cp Map - 90 mph');
    set(gca,'YDir','Reverse');
    xlabel('Streamwise Pressure Port Number');
    ylabel('Spanwise Pressure Port Number');
figure; contourf(RUN4_10);colorbar; title('RUN4 Cp Map - 100 mph');
    set(gca,'YDir','Reverse');
    xlabel('Streamwise Pressure Port Number');
    ylabel('Spanwise Pressure Port Number');
figure; contourf(RUN4_11);colorbar; title('RUN4 Cp Map - 110 mph');
    set(gca,'YDir','Reverse');
    xlabel('Streamwise Pressure Port Number');
    ylabel('Spanwise Pressure Port Number');
```

Pressure map - RUN 1 %

```
P1_1 = 11.92275316 * RUN1_1;
P1_2 = 47.69101262 * RUN1_2;
P1_3 = 107.3047784 * RUN1_3;
P1_4 = 190.7640505 * RUN1_4;
P1_5 = 298.0688289 * RUN1_5;
P1_6 = 429.2191136 * RUN1_6;
P1_7 = 584.2149046 * RUN1_7;
P1_8 = 763.056202  * RUN1_8;

figure; contourf(P1_1);colorbar; title('RUN1 Pressure (Pa) Map at 10 mph');
    set(gca,'YDir','Reverse');xlabel('Streamwise Pressure Port Number');
    ylabel('Spanwise Pressure Port Number');
figure; contourf(P1_2);colorbar; title('RUN1 Pressure (Pa) Map at 20 mph');
    set(gca,'YDir','Reverse');xlabel('Streamwise Pressure Port Number');
    ylabel('Spanwise Pressure Port Number');
figure; contourf(P1_3);colorbar; title('RUN1 Pressure (Pa) Map at 30 mph');
    set(gca,'YDir','Reverse');xlabel('Streamwise Pressure Port Number');
    ylabel('Spanwise Pressure Port Number');
figure; contourf(P1_4);colorbar; title('RUN1 Pressure (Pa) Map at 40 mph');
    set(gca,'YDir','Reverse');xlabel('Streamwise Pressure Port Number');
    ylabel('Spanwise Pressure Port Number');
figure; contourf(P1_5);colorbar; title('RUN1 Pressure (Pa) Map at 50 mph');
    set(gca,'YDir','Reverse');xlabel('Streamwise Pressure Port Number');
    ylabel('Spanwise Pressure Port Number');
figure; contourf(P1_6);colorbar; title('RUN1 Pressure (Pa) Map at 60 mph');
    set(gca,'YDir','Reverse');xlabel('Streamwise Pressure Port Number');
    ylabel('Spanwise Pressure Port Number');
figure; contourf(P1_7);colorbar; title('RUN1 Pressure (Pa) Map at 70 mph');
    set(gca,'YDir','Reverse');xlabel('Streamwise Pressure Port Number');
    ylabel('Spanwise Pressure Port Number');
figure; contourf(P1_8);colorbar; title('RUN1 Pressure (Pa) Map at 80 mph');
    set(gca,'YDir','Reverse');xlabel('Streamwise Pressure Port Number');
    ylabel('Spanwise Pressure Port Number');
```

Pressure Map - RUN 2 %

```
P2_1 = 11.92275316 * RUN2_1;
P2_2 = 47.69101262 * RUN2_2;
P2_3 = 107.3047784 * RUN2_3;
P2_4 = 190.7640505 * RUN2_4;
P2_5 = 298.0688289 * RUN2_5;
P2_6 = 429.2191136 * RUN2_6;
P2_7 = 584.2149046 * RUN2_7;
P2_8 = 763.056202  * RUN2_8;

figure; contourf(P2_1);colorbar; title('RUN2 Pressure (Pa) Map at 10 mph');
    set(gca,'YDir','Reverse');xlabel('Streamwise Pressure Port Number');
    ylabel('Spanwise Pressure Port Number');
figure; contourf(P2_2);colorbar; title('RUN2 Pressure (Pa) Map at 20 mph');
    set(gca,'YDir','Reverse');xlabel('Streamwise Pressure Port Number');
```

```
    ylabel('Spanwise Pressure Port Number');
figure; contourf(P2_3);colorbar; title('RUN2 Pressure (Pa) Map at 30 mph');
    set(gca,'YDir','Reverse');xlabel('Streamwise Pressure Port Number');
    ylabel('Spanwise Pressure Port Number');
figure; contourf(P2_4);colorbar; title('RUN2 Pressure (Pa) Map at 40 mph');
    set(gca,'YDir','Reverse');xlabel('Streamwise Pressure Port Number');
    ylabel('Spanwise Pressure Port Number');
figure; contourf(P2_5);colorbar; title('RUN2 Pressure (Pa) Map at 50 mph');
    set(gca,'YDir','Reverse');xlabel('Streamwise Pressure Port Number');
    ylabel('Spanwise Pressure Port Number');
figure; contourf(P2_6);colorbar; title('RUN2 Pressure (Pa) Map at 60 mph');
    set(gca,'YDir','Reverse');xlabel('Streamwise Pressure Port Number');
    ylabel('Spanwise Pressure Port Number');
figure; contourf(P2_7);colorbar; title('RUN2 Pressure (Pa) Map at 70 mph');
    set(gca,'YDir','Reverse');xlabel('Streamwise Pressure Port Number');
    ylabel('Spanwise Pressure Port Number');
figure; contourf(P2_8);colorbar; title('RUN2 Pressure (Pa) Map at 80 mph');
    set(gca,'YDir','Reverse');xlabel('Streamwise Pressure Port Number');
    ylabel('Spanwise Pressure Port Number');
```

Pressure Map - RUN 3 %

```
P3_1 = 11.92275316 * RUN3_1;
P3_2 = 47.69101262 * RUN3_2;
P3_3 = 107.3047784 * RUN3_3;
P3_4 = 190.7640505 * RUN3_4;
P3_5 = 298.0688289 * RUN3_5;
P3_6 = 429.2191136 * RUN3_6;
P3_7 = 584.2149046 * RUN3_7;
P3_8 = 763.056202  * RUN3_8;
P3_9 = 965.7430056 * RUN3_9;
P3_10 = 1192.275316 * RUN3_10;
P3_11 = 1442.653132 * RUN3_11;

figure; contourf(P3_1);colorbar; title('RUN3 Pressure Map (Pa) at 10 mph');
    set(gca,'YDir','Reverse');xlabel('Streamwise Pressure Port Number');
    ylabel('Spanwise Pressure Port Number');
figure; contourf(P3_2);colorbar; title('Run3 Pressure Map (Pa) at 20 mph');
    set(gca,'YDir','Reverse');xlabel('Streamwise Pressure Port Number');
    ylabel('Spanwise Pressure Port Number');
figure; contourf(P3_3);colorbar; title('RUN3 Pressure Map (Pa) at 30 mph');
    set(gca,'YDir','Reverse');xlabel('Streamwise Pressure Port Number');
    ylabel('Spanwise Pressure Port Number');
figure; contourf(P3_4);colorbar; title('RUN3 Pressure Map (Pa) at 40 mph');
    set(gca,'YDir','Reverse');xlabel('Streamwise Pressure Port Number');
    ylabel('Spanwise Pressure Port Number');
figure; contourf(P3_5);colorbar; title('RUN3 Pressure Map (Pa) at 50 mph');
    set(gca,'YDir','Reverse');xlabel('Streamwise Pressure Port Number');
    ylabel('Spanwise Pressure Port Number');
figure; contourf(P3_6);colorbar; title('RUN3 Pressure Map (Pa) at 60 mph');
    set(gca,'YDir','Reverse');xlabel('Streamwise Pressure Port Number');
    ylabel('Spanwise Pressure Port Number');
```

```
figure; contourf(P3_7);colorbar; title('RUN3 Pressure (Pa) Map at 70 mph');
    set(gca,'YDir','Reverse');xlabel('Streamwise Pressure Port Number');
    ylabel('Spanwise Pressure Port Number');
figure; contourf(P3_8);colorbar; title('RUN3 Pressure (Pa) Map at 80 mph');
    set(gca,'YDir','Reverse');xlabel('Streamwise Pressure Port Number');
    ylabel('Spanwise Pressure Port Number');
figure; contourf(P3_9);colorbar; title('RUN3 Pressure (Pa) Map at 90 mph');
    set(gca,'YDir','Reverse');xlabel('Streamwise Pressure Port Number');
    ylabel('Spanwise Pressure Port Number');
figure; contourf(P3_10);colorbar; title('RUN3 Pressure (Pa) Map at 100 mph');
    set(gca,'YDir','Reverse');xlabel('Streamwise Pressure Port Number');
    ylabel('Spanwise Pressure Port Number');
figure; contourf(P3_11);colorbar; title('RUN3 Pressure (Pa) Map at 110 mph');
    set(gca,'YDir','Reverse');xlabel('Streamwise Pressure Port Number');
    ylabel('Spanwise Pressure Port Number');
```

Pressure Map - RUN 4 %

```
P4_1 = 11.92275316 * RUN4_1;
P4_2 = 47.69101262 * RUN4_2;
P4_3 = 107.3047784 * RUN4_3;
P4_4 = 190.7640505 * RUN4_4;
P4_5 = 298.0688289 * RUN4_5;
P4_6 = 429.2191136 * RUN4_6;
P4_7 = 584.2149046 * RUN4_7;
P4_8 = 763.056202  * RUN4_8;
P4_9 = 965.7430056 * RUN4_9;
P4_10 = 1192.275316 * RUN4_10;
P4_11 = 1442.653132 * RUN4_11;

figure; contourf(P4_1);colorbar; title('RUN4 Pressure (Pa) Map at 10 mph');
    set(gca,'YDir','Reverse');xlabel('Streamwise Pressure Port Number');
    ylabel('Spanwise Pressure Port Number');
figure; contourf(P4_2);colorbar; title('RUN4 Pressure (Pa) Map at 20 mph');
    set(gca,'YDir','Reverse');xlabel('Streamwise Pressure Port Number');
    ylabel('Spanwise Pressure Port Number');
figure; contourf(P4_3);colorbar; title('RUN4 Pressure (Pa) Map at 30 mph');
    set(gca,'YDir','Reverse');xlabel('Streamwise Pressure Port Number');
    ylabel('Spanwise Pressure Port Number');
figure; contourf(P4_4);colorbar; title('RUN4 Pressure (Pa) Map at 40 mph');
    set(gca,'YDir','Reverse');xlabel('Streamwise Pressure Port Number');
    ylabel('Spanwise Pressure Port Number');
figure; contourf(P4_5);colorbar; title('RUN4 Pressure (Pa) Map at 50 mph');
    set(gca,'YDir','Reverse');xlabel('Streamwise Pressure Port Number');
    ylabel('Spanwise Pressure Port Number');
figure; contourf(P4_6);colorbar; title('RUN4 Pressure (Pa) Map at 60 mph');
    set(gca,'YDir','Reverse');xlabel('Streamwise Pressure Port Number');
    ylabel('Spanwise Pressure Port Number');
figure; contourf(P4_7);colorbar; title('RUN4 Pressure (Pa) Map at 70 mph');
    set(gca,'YDir','Reverse');xlabel('Streamwise Pressure Port Number');
    ylabel('Spanwise Pressure Port Number');
figure; contourf(P4_8);colorbar; title('RUN4 Pressure (Pa) Map at 80 mph');
```

```
    set(gca,'YDir','Reverse');xlabel('Streamwise Pressure Port Number');
    ylabel('Spanwise Pressure Port Number');
figure; contourf(P4_9);colorbar; title('RUN4 Pressure (Pa) Map at 90 mph');
    set(gca,'YDir','Reverse');xlabel('Streamwise Pressure Port Number');
    ylabel('Spanwise Pressure Port Number');
figure; contourf(P4_10);colorbar; title('RUN4 Pressure (Pa) Map at 100 mph');
    set(gca,'YDir','Reverse');xlabel('Streamwise Pressure Port Number');
    ylabel('Spanwise Pressure Port Number');
figure; contourf(P4_11);colorbar; title('RUN4 Pressure (Pa) Map at 110 mph');
    set(gca,'YDir','Reverse');xlabel('Streamwise Pressure Port Number');
    ylabel('Spanwise Pressure Port Number');
```

Velocity Map - RUN1 %

```
V1_1 = 10 * sqrt(1-RUN1_1);
V1_2 = 20 * sqrt(1-RUN1_2);
V1_3 = 30 * sqrt(1-RUN1_3);
V1_4 = 40 * sqrt(1-RUN1_4);
V1_5 = 50 * sqrt(1-RUN1_5);
V1_6 = 60 * sqrt(1-RUN1_6);
V1_7 = 70 * sqrt(1-RUN1_7);
V1_8 = 80 * sqrt(1-RUN1_8);

figure; contourf(V1_1);colorbar; title('RUN1 velocity Map - 10 mph');
    set(gca,'YDir','Reverse');xlabel('Streamwise Pressure Port Number');
    ylabel('Spanwise Pressure Port Number');
figure; contourf(V1_2);colorbar; title('RUN1 Velocity Map - 20 mph');
    set(gca,'YDir','Reverse');xlabel('Streamwise Pressure Port Number');
    ylabel('Spanwise Pressure Port Number');
figure; contourf(V1_3);colorbar; title('RUN1 Velocity Map - 30 mph');
    set(gca,'YDir','Reverse');xlabel('Streamwise Pressure Port Number');
    ylabel('Spanwise Pressure Port Number');
figure; contourf(V1_4);colorbar; title('RUN1 Velocity Map - 40 mph');
    set(gca,'YDir','Reverse');xlabel('Streamwise Pressure Port Number');
    ylabel('Spanwise Pressure Port Number');
figure; contourf(V1_5);colorbar; title('RUN1 Velocity Map - 50 mph');
    set(gca,'YDir','Reverse');xlabel('Streamwise Pressure Port Number');
    ylabel('Spanwise Pressure Port Number');
figure; contourf(V1_6);colorbar; title('RUN1 Velocity Map - 60 mph');
    set(gca,'YDir','Reverse');xlabel('Streamwise Pressure Port Number');
    ylabel('Spanwise Pressure Port Number');
figure; contourf(V1_7);colorbar; title('RUN1 Velocity Map - 70 mph');
    set(gca,'YDir','Reverse');xlabel('Streamwise Pressure Port Number');
    ylabel('Spanwise Pressure Port Number');
figure; contourf(V1_8);colorbar; title('RUN1 Velocity Map - 80 mph');
    set(gca,'YDir','Reverse');xlabel('Streamwise Pressure Port Number');
    ylabel('Spanwise Pressure Port Number');
```

Velocity Map - RUN2 %

```
V2_1 = 10 * sqrt(1-RUN2_1);
V2_2 = 20 * sqrt(1-RUN2_2);
V2_3 = 30 * sqrt(1-RUN2_3);
V2_4 = 40 * sqrt(1-RUN2_4);
V2_5 = 50 * sqrt(1-RUN2_5);
V2_6 = 60 * sqrt(1-RUN2_6);
V2_7 = 70 * sqrt(1-RUN2_7);
V2_8 = 80 * sqrt(1-RUN2_8);

figure; contourf(V2_1);colorbar; title('RUN2 Velocity Map - 10 mph');
    set(gca,'YDir','Reverse');xlabel('Streamwise Pressure Port Number');
    ylabel('Spanwise Pressure Port Number');
figure; contourf(V2_2);colorbar; title('RUN2 Velocity Map - 20 mph');
    set(gca,'YDir','Reverse');xlabel('Streamwise Pressure Port Number');
    ylabel('Spanwise Pressure Port Number');
figure; contourf(V2_3);colorbar; title('RUN2 Velocity Map - 30 mph');
    set(gca,'YDir','Reverse');xlabel('Streamwise Pressure Port Number');
    ylabel('Spanwise Pressure Port Number');
figure; contourf(V2_4);colorbar; title('RUN2 Velocity Map - 40 mph');
    set(gca,'YDir','Reverse');xlabel('Streamwise Pressure Port Number');
    ylabel('Spanwise Pressure Port Number');
figure; contourf(V2_5);colorbar; title('RUN2 Velocity Map - 50 mph');
    set(gca,'YDir','Reverse');xlabel('Streamwise Pressure Port Number');
    ylabel('Spanwise Pressure Port Number'); grid on;grid minor;
figure; contourf(V2_6);colorbar; title('RUN2 Velocity Map - 60 mph');
    set(gca,'YDir','Reverse');xlabel('Streamwise Pressure Port Number');
    ylabel('Spanwise Pressure Port Number'); grid on;grid minor;
figure; contourf(V2_7);colorbar; title('RUN2 Velocity Map - 70 mph');
    set(gca,'YDir','Reverse');xlabel('Streamwise Pressure Port Number');
    ylabel('Spanwise Pressure Port Number'); grid on;grid minor;
figure; contourf(V2_8);colorbar; title('RUN2 velocity Map - 80 mph');
    set(gca,'YDir','Reverse');xlabel('Streamwise Pressure Port Number');
    ylabel('Spanwise Pressure Port Number'); grid on;grid minor;
```

Velocity Map - RUN3 %

```
V3_1 = 10 * sqrt(1-RUN3_1);
V3_2 = 20 * sqrt(1-RUN3_2);
V3_3 = 30 * sqrt(1-RUN3_3);
V3_4 = 40 * sqrt(1-RUN3_4);
V3_5 = 50 * sqrt(1-RUN3_5);
V3_6 = 60 * sqrt(1-RUN3_6);
V3_7 = 70 * sqrt(1-RUN3_7);
V3_8 = 80 * sqrt(1-RUN3_8);
V3_9 = 90 * sqrt(1-RUN3_9);
V3_10 = 100 * sqrt(1-RUN3_10);
V3_11 = 110 * sqrt(1-RUN3_11);

figure; contourf(V3_1);colorbar; title('RUN3 Velocity Map - 10 mph');
    set(gca,'YDir','Reverse');xlabel('Streamwise Pressure Port Number');
    ylabel('Spanwise Pressure Port Number');
figure; contourf(V3_2);colorbar; title('RUN3 Velocity Map - 20 mph');
```

```
    set(gca,'YDir','Reverse');xlabel('Streamwise Pressure Port Number');
    ylabel('Spanwise Pressure Port Number');
figure; contourf(V3_3);colorbar; title('RUN3 Velocity Map - 30 mph');
    set(gca,'YDir','Reverse');xlabel('Streamwise Pressure Port Number');
    ylabel('Spanwise Pressure Port Number');
figure; contourf(V3_4);colorbar; title('RUN3 Velocity Map - 40 mph');
    set(gca,'YDir','Reverse');xlabel('Streamwise Pressure Port Number');
    ylabel('Spanwise Pressure Port Number');
figure; contourf(V3_5);colorbar; title('RUN3 Velocity Map - 50 mph');
    set(gca,'YDir','Reverse');xlabel('Streamwise Pressure Port Number');
    ylabel('Spanwise Pressure Port Number');
figure; contourf(V3_6);colorbar; title('RUN3 Velocity Map - 60 mph');
    set(gca,'YDir','Reverse');xlabel('Streamwise Pressure Port Number');
    ylabel('Spanwise Pressure Port Number');
figure; contourf(V3_7);colorbar; title('RUN3 Velocity Map - 70 mph');
    set(gca,'YDir','Reverse');xlabel('Streamwise Pressure Port Number');
    ylabel('Spanwise Pressure Port Number'); grid on;grid minor;

figure; contourf(V3_8);colorbar; title('RUN3 Velocity Map - 80 mph');
    set(gca,'YDir','Reverse');xlabel('Streamwise Pressure Port Number');
    ylabel('Spanwise Pressure Port Number'); grid on;grid minor;
figure; contourf(V3_9);colorbar; title('RUN3 Velocity Map - 90 mph');
    set(gca,'YDir','Reverse');xlabel('Streamwise Pressure Port Number');
    ylabel('Spanwise Pressure Port Number'); grid on;grid minor;
figure; contourf(V3_10);colorbar; title('RUN3 Velocity Map - 100 mph');
    set(gca,'YDir','Reverse');xlabel('Streamwise Pressure Port Number');
    ylabel('Spanwise Pressure Port Number'); grid on;grid minor;
figure; contourf(V3_11);colorbar; title('RUN3 Velocity Map - 110 mph');
    set(gca,'YDir','Reverse');xlabel('Streamwise Pressure Port Number');
    ylabel('Spanwise Pressure Port Number'); grid on;grid minor;
```

Velocity Map - RUN4 %

```
V4_1 = 10 * sqrt(1-RUN4_1);
V4_2 = 20 * sqrt(1-RUN4_2);
V4_3 = 30 * sqrt(1-RUN4_3);
V4_4 = 40 * sqrt(1-RUN4_4);
V4_5 = 50 * sqrt(1-RUN4_5);
V4_6 = 60 * sqrt(1-RUN4_6);
V4_7 = 70 * sqrt(1-RUN4_7);
V4_8 = 80 * sqrt(1-RUN4_8);
V4_9 = 90 * sqrt(1-RUN4_9);
V4_10 = 100 * sqrt(1-RUN4_10);
V4_11 = 110 * sqrt(1-RUN4_11);

figure; contourf(V4_1);colorbar; title('RUN4 Velocity Map - 10 mph');
    set(gca,'YDir','Reverse');xlabel('Streamwise Pressure Port Number');
    ylabel('Spanwise Pressure Port Number');
figure; contourf(V4_2);colorbar; title('RUN4 Velocity Map - 20 mph');
    set(gca,'YDir','Reverse');xlabel('Streamwise Pressure Port Number');
    ylabel('Spanwise Pressure Port Number');
figure; contourf(V4_3);colorbar; title('RUN4 Velocity Map - 30 mph');
    set(gca,'YDir','Reverse');xlabel('Streamwise Pressure Port Number');
```

```
    ylabel('Spanwise Pressure Port Number');
figure; contourf(v4_4);colorbar; title('RUN4 Velocity Map - 40 mph');
    set(gca,'YDir','Reverse');xlabel('Streamwise Pressure Port Number');
    ylabel('Spanwise Pressure Port Number');
figure; contourf(v4_5);colorbar; title('RUN4 Velocity Map - 50 mph');
    set(gca,'YDir','Reverse');xlabel('Streamwise Pressure Port Number');
    ylabel('Spanwise Pressure Port Number');
figure; contourf(v4_6);colorbar; title('RUN4 Velocity Map - 60 mph');
    set(gca,'YDir','Reverse');xlabel('Streamwise Pressure Port Number');
    ylabel('Spanwise Pressure Port Number');
figure; contourf(v4_7);colorbar; title('RUN4 Velocity Map - 70 mph');
    set(gca,'YDir','Reverse');xlabel('Streamwise Pressure Port Number');
    ylabel('Spanwise Pressure Port Number');
figure; contourf(v4_8);colorbar; title('RUN4 Velocity Map - 80 mph');
    set(gca,'YDir','Reverse');xlabel('Streamwise Pressure Port Number');
    ylabel('Spanwise Pressure Port Number');
figure; contourf(v4_9);colorbar; title('RUN4 Velocity Map - 90 mph');
    set(gca,'YDir','Reverse');xlabel('Streamwise Pressure Port Number');
    ylabel('Spanwise Pressure Port Number');
figure; contourf(v4_10);colorbar; title('RUN4 Velocity Map - 100 mph');
    set(gca,'YDir','Reverse');xlabel('Streamwise Pressure Port Number');
    ylabel('Spanwise Pressure Port Number');
figure; contourf(v4_11);colorbar; title('RUN4 Velocity Map - 110 mph');
    set(gca,'YDir','Reverse');xlabel('Streamwise Pressure Port Number');
    ylabel('Spanwise Pressure Port Number');
```

Published with MATLAB® R2014a

Appendix ii

Experiment Iterations:

Iteration 1:

The first iteration of this experiment was conducted in the University of Washington's Low Speed Wind tunnel (LWT)[22]. The plate and the vortex generators were 3D printed and tested for different speeds of the tunnel. There were 5 types of VGs used as follows: h = height, angle = angle of attack

1. VG1 (h = 20 mm angle = 45 deg)
2. VG2 (h = 15 mm angle = 45 deg)
3. VG3 (h = 15 mm angle = 25 deg)
4. VG4 (h = 15 mm angle = 55 deg)
5. VG5 (h = 15 mm angles = 45 deg 45 deg) symmetric trapezoidal

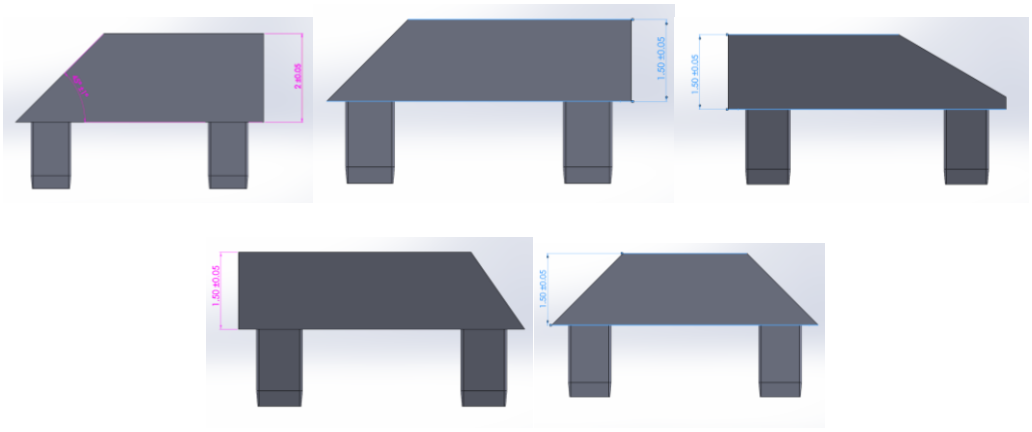

Fig A-ii.1: VGs used for iterations 1 & 2. Top Row - VG1 (h = 20 mm angle = 45 deg), VG2 (h = 15 mm angle = 45 deg), VG3 (h = 15 mm angle = 25 deg) Bottom Row: VG4 (h = 15 mm angle = 55 deg), VG5 (h = 15 mm angles = 45 deg 45 deg) symmetric trapezoidal

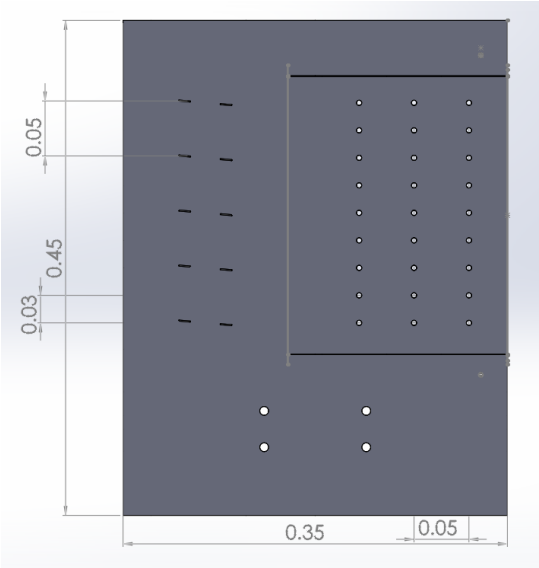

Fig A-ii.2: Flat Plate used in Iterations 1 & 2

The VGs were inserted in the angled slots for each run and could be removed and interchanged as desired. For each type of VGs, the following test runs were conducted:

1. All 5 VGs mounted on the plate at a yaw angle of -5 degrees
2. One central VG mounted on the plate at a yaw angle of -5 degrees
3. A ‘no VG’ case was also run for flow calibration without any disturbances.

The pressure sensors used in this iteration were not sensitive enough to obtain the desired results and therefore the iteration was unsuccessful.

Iteration 2:

Iteration 2 used the same VG and plate configuration but the testes were held at the Kirsten Wind Tunnel (KWT). The more sensitive EPS pressure sensor system was used and the results obtained were more conclusive than the iteration 1.

Fig A-ii.3: Plate with 5 VGs mounted in KWT for Iteration 2: Front view

Fig A-ii.4: Plate with 1 central VG mounted in KWT for Iteration 2: Front view

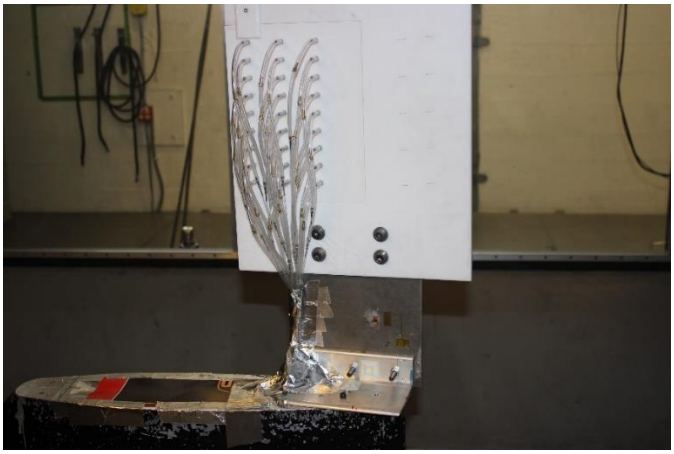

Fig A-ii.5: Plate connected to KWT EPS System

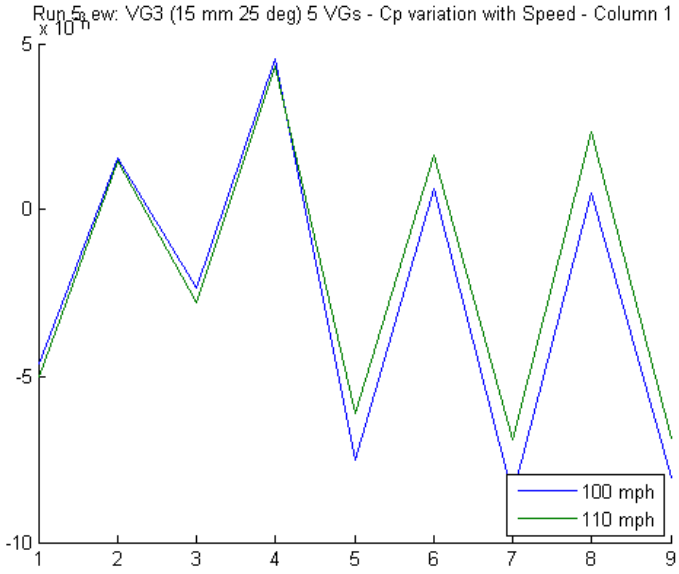

Fig A-ii.6 The *Cp* plot for the speed variation at column nearest to VGs for all 5 VGs mounted. There *Cp* value dips can be observed

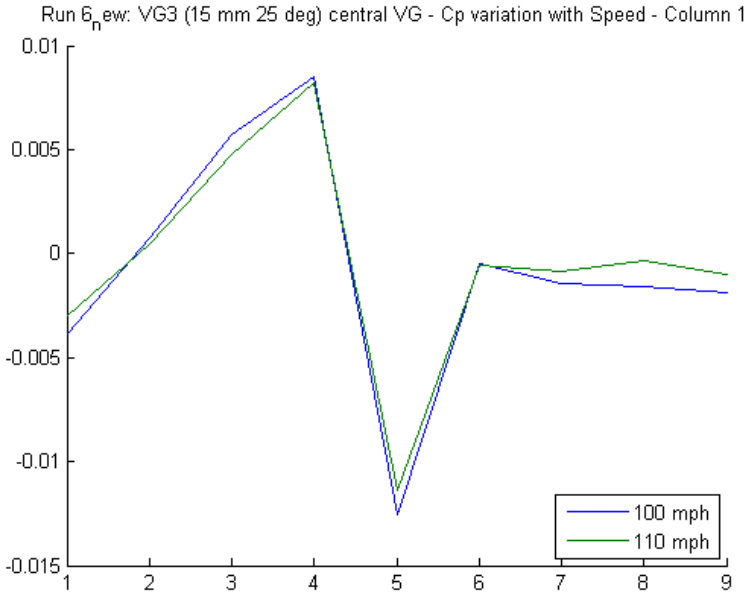

Fig A-ii.6 The *Cp* plot for the speed variation at column nearest to VGs for 1 central VG mounted. Only 1 *Cp* value dip is observed

The results showed very low negative values of pressure coefficient indicating presence of weak vortices. The VG height was lesser than what it should have been. Also, the port arrangement on the plate was too scarce to predict the flow map over the plate. In this iteration, only 27 pressure ports were used on the plate. The iteration 3 used a bigger plate to accommodate 63 ports laid closer together. The VG height was also increased to 1 inch i.e. 25.4 mm.